Multi-Scale Seismic Fragility and Performance Assessment of the Thjórsá-Bridge under Evolving Icelandic Design Standards

Ching-Yi Tsai

Bjarni Bessason

Vegagerðin

HÍ | UMHVERFIS- OG BYGGINGARVERKFRÆÐIDEILD

April 2026

A research project supported by grant from
Icelandic Road and Coastal Administration Research Fund
grant nr. 1800-1029

Table of Contents

Abstract

This research presents a multi-scale seismic fragility and performance assessment of the Thjórsá Bridge, a vital infrastructure asset in the high-seismicity region of South Iceland. The study focuses on the vulnerability of the Lead-Rubber Bearing (LRB) isolation system using an analytical framework that reconciles global system-level responses with localized component-level demands.

A comprehensive Nonlinear Time History Analysis (NLTHA) was conducted using a suite of nine ground motion records from the 2000 and 2008 South Iceland earthquakes, scaled to Eurocode 8 (EC8) Type A response spectra. To evaluate structural sensitivity, two modelling configurations—"Pinned" (moment end-releases) and "Fixed" (rigid connections)—were examined. Furthermore, the records were partitioned into two directional groups to isolate the effects of longitudinal-dominant (Group 1) versus transverse-dominant (Group 2) excitations.

The resulting fragility curves identify Group 2 (Transverse) motions as the governing demand case, revealing a high sensitivity in the arch-deck anchorage system. Comparative analysis between the 2002 and 2010 Icelandic National Annexes demonstrates a significant increase in seismic risk; the shift in design acceleration to 0.5g moves the bridge into a regime with a high probability of exceeding serviceability damage states. Conversely, a Pier Moment Capacity Check utilizing the Mander confined concrete model confirms that the substructure remains within the elastic range at design-level intensities, validating the effectiveness of the LRBs in protecting primary vertical members.

The findings provide a robust template for the seismic risk management of isolated bridges in Iceland, emphasizing the critical role of ground motion directionality and evolving design standards in the life-cycle assessment of modern infrastructure.

Keywords: Seismic Fragility, Lead-Rubber Bearings, Arch Bridge, Icelandic Design Codes, Nonlinear Time History Analysis, Multi-Scale Assessment.

Ágrip á Íslensku

Markmið rannsóknaverkefnis er að þróa og aðlaga aðferðafræði til að meta tjónnæmi brúa gagnvart jarðaskjálftaáraun og með því leggja grunn að áhættugreiningu á mikilvægum innviðum á brotabelti Suðurlands. Þjórsárbrúin á Þjóðvegi 1 er notuð sem tilvik í rannsókninni.

Þjórsárbrúin var byggð árið 2004. Hún er mikilvægt samgöngumannvirki á Suðurlandi og það eru langar hjáleiðir ef hún skemmist og verður óökufær í jarðskjálfta. Brúin er 170 metra löng og samanstendur af einum 78 metra víðum boga, sjö millistöplum og tveimur landstöplum, sem saman bera yfirbygginguna (brúardekkið). Bogi og yfirbygging eru hönnuð sem samverkandi stál-steypuþversnið. Yfirbyggingin er steypt föst við efsta hluta bogans og því reynir mikið á bogann og grundun hans í kröftugum jarðskjálftum. Ofan á alla stöpla eru blýgúmmílegur sem draga úr áraun á þá. Áherslan í þessu verkefni takmarkast við að meta tjónnæmi leganna en einnig er áraun neðst í stöplum skoðuð. Notað er tölulegt reiknilíkan þar sem gert er ráð fyrir að allar einingar í líkaninu séu á línulegu fjaðursviði nema einingarnar sem herma legurnar. Fyrir þær er notast við sérstakar ólínulegar tengieiningar, en hönnun þeirra miðast við að þær fari á flotsvið við kröftuga jarðskjálftaáraun sem takmarkar áraun á stöplana. Til að meta næmni mannvirkisins eru skoðuð tvö tölvulíkön, liðtengdir og stífar tengingar fyrir þverbita.

Tjónnæmi burðarvirkisins er metið með ólínulegri tímaraðagreiningu. Valdar eru níu tímaraðir sem skráðar voru í Suðurlandsskjálftunum árið 2000 og 2008. Tímaraðirnar eru kvarðaðar með sérstökum hætti út frá jarðskjálftarófi Eurocode 8 og þannig tengdar við hönnunarröðun staðalsins. Tímaröðunum var beitt á brúarlíkanið með stigvaxandi ákefð (*Icremental Dynamic Analysis*). Ákvarðaðir voru skemmdaferlar þar sem kröftugri lárétti stefnuþáttur tímaraðanna verkar annars vegar í langátt brúar og sá veikar í þverátt, og hins vegar þar sem kröftugri stefnuþátturinn verkar í þverátt og hinn í langátt. Í hvoru tilviki er skeraflögun lega í bæði lang- og þverátt skoðuð. Greiningin leiðir í ljós að aðaláraun í þverátt og svörun í þverátt er krítískust fyrir legurnar.

Jarðskjálftaálag á brotabelti Suðurlands jókst verulega þegar þjóðarskjölunum frá 2002 og skipt út með þjóðarviðaukum 2010. Bæði hækkaði hönnunarhröðunin frá 0,4g í 0,5g og einnig var einum rófstuðli (Tc) fyrir jarðvegsflokk A (klöpp) breytt til að taka betur tillit til nærsprunguáhrifa. Seinni atriðið eykur álag fyrir mannvirki með langa sveiflutíma. Ef miðað er við núgildandi staðalálag fyrir svæðið (PGA=0.5g) eru miklar líkur á að tveir fyrstu skemmdaferlarnir (DS1 og DS2) verði yfirstignir fyrir þverstefnuna. Hins vegar staðfestir athugunin að beygjuvægisáraun á stöpla er vel innan fjaðursviðsmarka fyrir þetta álag, sem staðfestir virkni blýgúmmíleganna við að vernda undirstöðurnar.

Niðurstöðurnar þjóna sem grunnur fyrir jarðskálftaáhættumat á Þjórsárbrúni. Tilsvarandi skemmdaferla þarf svo að reikna fyrir aðra krítíska staði í brúnni. Aðferðafræðina má svo heimafæra við áhættugreiningu á öðrum brúm.

Lykilorð: Jarðskjálftatjónæmi, blýgúmmílegur, bogabrú, íslenskir hönnunarstaðlar, ólínuleg tímaraðagreining, fjölþátta greining.

1 Introduction

The objective of this research project is to develop and adapt a methodology for assessing the seismic vulnerability of bridges and thereby establish a basis for risk assessment of critical infrastructure in the South Iceland Seismic Zone (SISZ). The Thjórsá-Bridge on Highway 1 in Iceland is used as a case study in this project (Figure 1).

The bridge was built in 2004. It is an important transportation structure in South Iceland, and detours are long if it is damaged and becomes impassable in a destructive earthquake. Figure 2 shows its location in the middle of the SISZ and its proximity to the South Iceland earthquakes of June 2000 and May 2008. Station locations of the Icelandic Strong-motion network of the Earthquake Engineering Research Institute of University of Iceland are also shown in the figure.

The Thjórsá-bridge is 170 meters long. It consists of a single 78-meter-wide arch spanning the river and partly supporting the superstructure (the bridge deck) with a wall connection at the middle of the arch and with two piers. In addition, there are five piers and two abutments supporting the remaining part of the superstructure (Figure 1). The arch and the superstructure are designed as a composite steel–concrete cross-section. The superstructure is cast integrally with the top central part of the arch, whilst on the top of the piers and abutments lead–rubber bearings are installed that reduce the seismic demands on the piers. The arch therefore largely controls the displacement of the superstructure, especially in the longitudinal direction. The arc and its foundations are consequently subjected to strong seismic forces. Rock anchors are used fix the arch ends to the ground.

Figure 1 *– The Thjórsá-Bridge on Highway 1 in Iceland, build in 2004.*

The focus of this project is limited to assessing the seismic vulnerability of the bearings in the bridge and partly the piers protected by the bearings. Assessment of the vulnerability of the arch and its rock anchors are not covered in this study. The same numerical model and methodology can nevertheless be used to evaluate the vulnerability of the arch and other load-bearing components and critical cross-sections of the bridge.

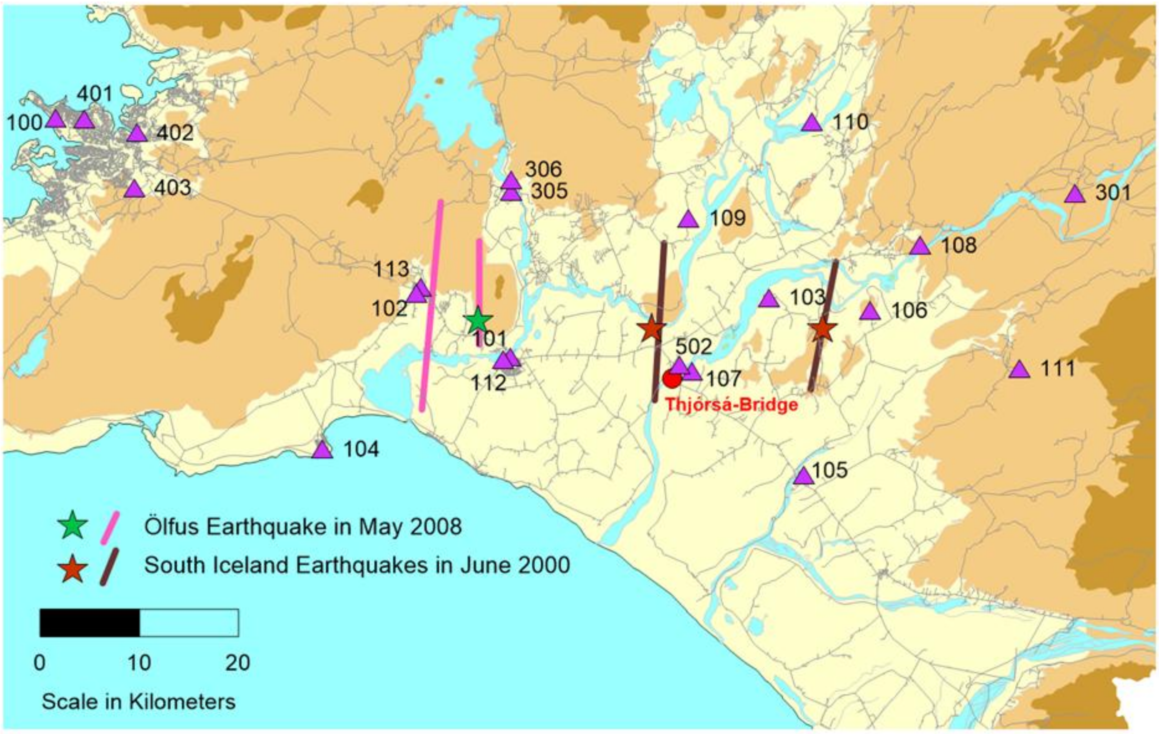

***Figure 2** – Location of the Thjórsá-Bridge in the South Iceland Seismic Zone and the epicentre and fault rupture of the South Iceland earthquake in June 2000 and the Ölfus earthquake in May 2008. Locations of stations in the Icelandic strong motion network in South Iceland are shown with △ and their Id. numbers.*

2 Methodology

Incremental dynamic analysis (IDA) is a well-known method for seismic vulnerability assessment. The approach demands scaled ground motion acceleration time histories. When available it is preferable to use recorded local time histories. A special technic is needed to scale the time histories. Demand parameters are used to define damage states. In the following sections these topics are addressed.

2.1 Incremental dynamic analysis

The Incremental dynamic analysis is used to evaluate the seismic performance of structures (Vamvatsikos & Cornell, 2002). In IDA, a structure is subjected to a suite of ground motion records that are progressively scaled in intensity. For each scaling step, a nonlinear time-history analysis is performed, and the structural demand (e.g., maximum drift, base shear, damage indices) are recorded at predefined locations and critical sections.

By plotting the selected response parameters versus intensity measure IDA curves are obtained. The intensity measure (IM) can be defined in several ways. It is common to use the peak ground acceleration (PGA) as IM, but also different parameters based on the acceleration response spectra $S_a(T)$ for the suite of ground motion records used in the IDA. Often the ordinate for the fundamental period, T_1, is used, $S_a(T_1)$, or some average value from the response spectra for period bin around $S_a(T_1)$. The IDA curves provide insight into both elastic and inelastic behaviour, up to potential failure or collapse.

IDA is widely used because it captures; the full range of structural response, from elastic to nonlinear response and collapse; record-to-record variability in seismic demand; and probabilistic information for fragility and performance assessment.

An alternative to apply IDA is to use a "cloud analysis" where the time histories have their natural intensity. Each non-linear time history analysis of unscaled time series gives one point, i.e. computed engineering demand parameter versus selected intensity parameter. The result is a scatter plot ("cloud"), which serves as the basis for fitting a probabilistic model from which fragility curves are derived. The cloud analysis is not used in this report.

2.2 Selection of ground motion records

For the IDA-method, it is necessary to select and suit of acceleration time histories to use in the study. Local records are preferred when available. A width of strong motion data was recorded in the three South Iceland earthquakes in June 2000 and May 2008. The first one, the *Holt earthquake* was largest. It struck on 17th of June 2000 and was of moment magnitude M_w6.5. The second one was the *Hestfjall earthquake* which was on 21st of June 2000 and was M_w6.4, and finally the *Ölfus earthquake* on 29th of May 2008 which was M_w6.3 (Jónasson et al. 2021; Jónasson et al. 2024). Stations in the South Iceland strong motion network are shown on Figure 2 along with location of the Thjórsá-Bridge. Some stations, like 502 and 107 are very close to the bridge site and are therefore important to reflect expected seismic loads and the site.

In this analysis nine sets of records will be used, three from each event mentioned above. The selected records are listed up in Table 1. All the sets were recorded at close distance to the epicentre, R_{Epi} and close to the fault rupture with short Joyner Boore distance, R_{JB}, as shown in the two last columns. The recorded peak ground acceleration (PGA) for the larger horizontal component is above 0.3g in all cases and above 0.5g in seven cases.

In Figure 3, the response spectra for the unscaled two horizonal components of these nine sets of records are compared to the EC8-1 spectrum for the site where the reference peak ground acceleration (a_{gR}) with 475 year mean return period is read from the seismic hazard map in the Icelandic National Annexes with the Eurocodes (SI, 2010) (a_{gR} =0.5g, Ground type A, γ_I=1.0, T_C=0.5) for 5% damping ratio.

***Table 1** – Recorded PGA in the June 2000 South Iceland earthquake and the May 2008 Ölfus earthquake, for the horizontal components X and Y and the vertical component Z.* The larger PGA for the two horizontal components is shown each case with bold font.

Event	Id	Station	Soil class	PGA_X (g)	PGA_Y (g)	PGA_Z (g)	R_{Epi} [1] (km)	R_{JB} [2] (km)
Holt	105	Hella	Cemented sand	0.208	**0.477**	0.182	15	7
17.06.2000	106	Flagbjarnarholt	Rock	0.318	**0.338**	0.273	5	4
M_w=6.50	103	Kaldárholt	Rock	**0.625**	0.512	0.667	6	6
Hestfjall	502	Thjórsár Bridge (W)	Lava /sediments	0.744	**0.838**	0.422	5	3
21.06.2000	107	Thjórsártún	Rock	0.529	**0.568**	0.325	6	3
M_w=6.42	109	Sólheimar í Grímsnesi	Sediments	0.420	**0.721**	0.420	12	5
Ölfus	113	Hveragerði, Ás	Rock	**0.664**	0.468	0.437	6.5	2
29.05.2008	112	Selfoss city hall	Rock	**0.536**	0.326	0.251	5	3
M_w=6.29	101	Selfoss hospital	Rock	**0.509**	0.217	0.180	5	3

1) R_{Epi} – Epicentral distance.
2) R_{JB} – Joyner Boore distance.

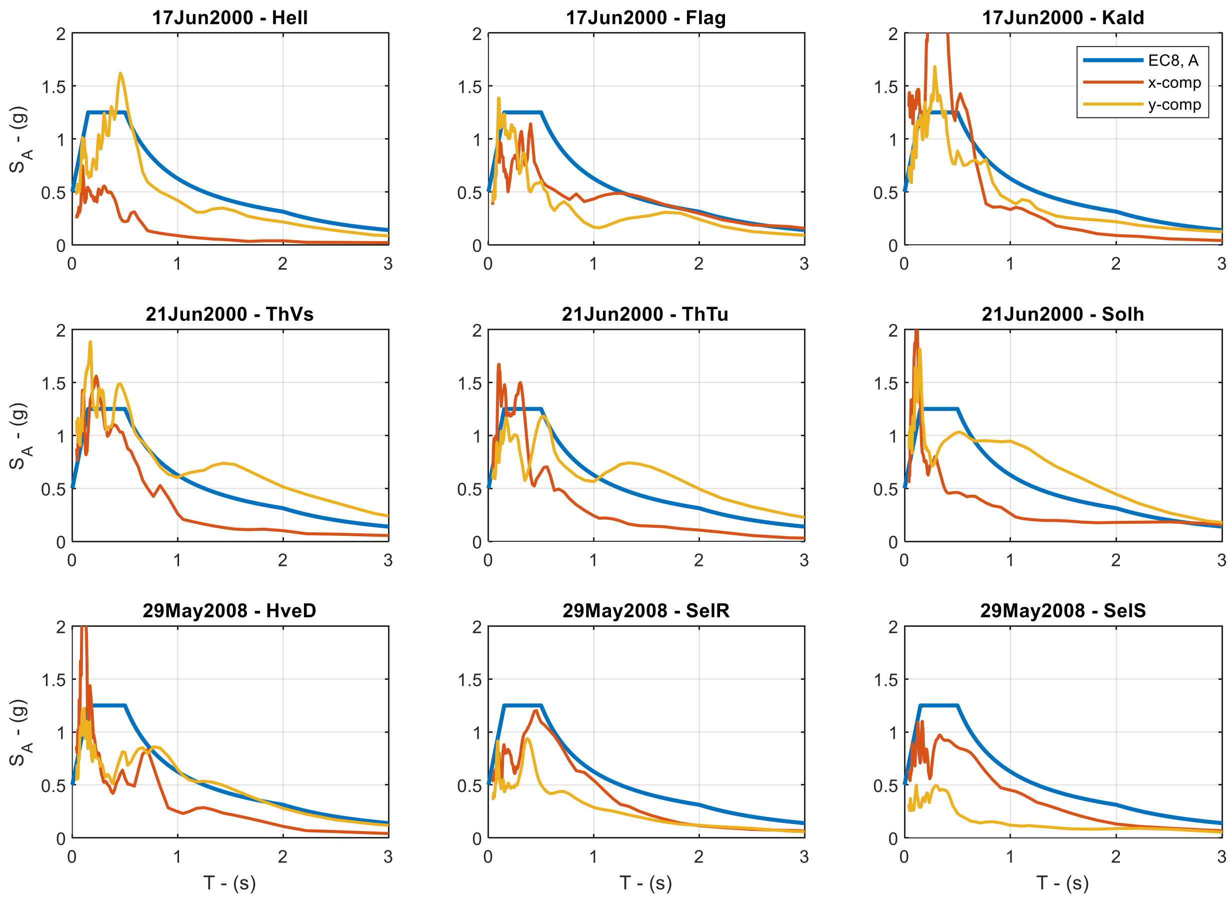

***Figure 3** – Unscaled response spectra from the 17 June 2000, 21 June 2000 and 29 May 2008 earthquakes for all the stations listed up in Table 1.*

2.3 Scaling of time histories

Number of calibration methods exist. In Eurocode 8 Part 1 (EC8-1) for buildings (CEN, 2004) one approach is given, and then in the Eurocode 8 Part 2 (EC8-2) for bridges (CEN, 2005) another version is given. In the next generation of the Eurocodes one more scaling method is now under review. Here, the EC8-1 method will be used to scale recorded acceleration time histories from recent South Iceland earthquakes. At each station three components are available, two horizontal (x- and y-components) and one vertical component (z-component). Records, from three stations, in each earthquake (17 June 2000, 21 June 2000, and 29 May 2008) will be used (Table 1). The horizontal component with the larger intensity in the period range T=0 to T=2.5s will be used for the scaling. The intensity is computed as:

$$I_{SA} = \int_{0}^{2.5s} S_A(T,\xi)dT \qquad (1)$$

where $S_A(T,\xi)$ is the acceleration response spectrum for a given component and the damping ratio, here ξ=5%. Table 2 shows the selected time histories and the component with the higher intensity.

***Table 2** – Selected time histories (unscaled) from stations in the South Iceland seismic zone.*

No.	Date	Earth quake	M_w	Station	Dist.[1] (km)	Com-ponent	PGA (g)	I_{SA} (gs)
1	17.06.2000	Holt	6.52	Hella	3	y	0.48	1.21
2	17.06.2000	Holt	6.52	Kaldhárholt	6	x	0.63	1.46
3	17.06.2000	Holt	6.52	Flagbjarnarholt	3	x	0.32	1.14
4	21.06.2000	Hestfjall	6.44	Thjórsárbrú VS	3	y	0.84	1.91
5	21.06.2000	Hestfjall	6.44	Thjórsártún	3	y	0.57	1.64
6	21.06.2000	Hestfjall	6.44	Sólheimar	5	y	0.72	1.81
7	29.05.2008	Ölfus	6.31	Selfoss – City hall	3	x	0.54	1.10
8	29.05.2008	Ölfus	6.31	Hveragerdi – Residense hall	2	y	0.47	1.31
9	29.05.2008	Ölfus	6.31	Selfoss – Hospital	3	x	0.51	1.03

1) Joyner Boore distance

To scale the set of the selected time histories so they match the Eurocode 8 response spectrum shown it is necessary to define a reference natural period, T_{ref}. The period range, $0.2T_{ref}$ to $2.0T_{ref}$ is then used in the scaling. For building, T_{ref} is commonly the fundamental natural period, i.e. $T_{ref}=T_1$ but for complex 3D structure like bridge the T_{ref} is usually related to the modes with the largest mass participation for either the longitudinal axis or the transverse axis of the bridge.

The scaling procedure is carried out in four steps:

1. A multiplier, M_{1i}, is found so the intensity of the selected response spectrum for time history, *i,* (see Table 2), in the period range $0.2T_{ref}$ to $2.0T_{ref}$ is equal to the intensity of the EC8 response spectrum in the same range, using Eq.(1) but integrating over the interval $0.2T_{ref}$ to $2.0T_{ref}$.

2. Each selected response spectra is scaled with its M_{1i}-factor and then a mean spectrum is computed for all the nine components.
3. The mean spectrum is scaled with a factor M2 to ensure that it is above the 90% level of the EC8 target response spectrum for all ordinates in the period range $0.2T_{ref}$ to $2.T_{ref}$.
4. The final step is to combine the two multipliers, i.e. M_{1i} and M_2, and compute the M_i multiplier for each time history is found:

$$M_i = M_{1i} \times M_2 \qquad (2)$$

Figure 4 shows as an example how M_{1i} is computed for the first record in Table 1 for T_{ref}=0.5s and the period range therefore [0.1s, 1.0s]. The target EC8-1 response spectrum has $a_g = \gamma_I \cdot a_{gR} = 1.3 \cdot 0.5 = 0.65g$. The response spectrum for the time history is unscaled in Figure 4a while in Figure 4b the M_{1i} has been used to scale the spectrum, so it matches the target spectrum. Figure 5a then shows the mean response spectrum for all the 9 selected time histories after each of them has been scaled with M_{1i} and Figure 5b shows how M_2 is found to ensure that all ordinates are above the 90% level of the EC8-1 target spectrum. Table 3 shows the results for all the time histories in Table1 for the T_{ref}=0.5s. PGA values are shown before and after scaling.

***Table 3** – Scaling factors for the selected time histories for T_{ref}=0.50s.*

No.	Date	Station	Unscaled PGA (g)	M_{1i}	M_2	$M_i= M_{1i}\times M_2$	Scaled PGA (g)
1	17.06.2000	HELL	0.48	1.549	1.085	**1.680**	0.81
2	17.06.2000	KALD	0.63	1.053	1.085	**1.142**	0.72
3	17.06.2000	FLAG	0.32	2.143	1.085	**2.324**	0.74
4	21.06.2000	THBR	0.84	1.235	1.085	**1.339**	1.12
5	21.06.2000	THTU	0.57	1.612	1.085	**1.749**	1.00
6	21.06.2000	SOLH	0.72	1.361	1.085	**1.476**	1.06
7	29.05.2008	SELR	0.54	1.597	1.085	**1.733**	0.94
8	29.05.2008	HVED	0.47	1.734	1.085	**1.881**	0.88
9	29.05.2008	SELS	0.51	1.799	1.085	**1.952**	1.00
		Mean:	0.56			Mean:	0.91

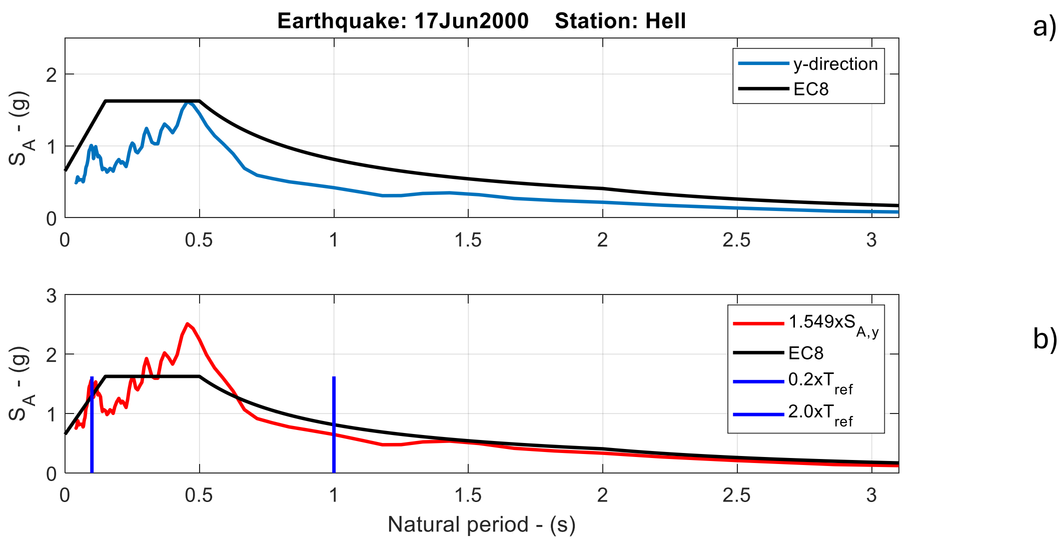

***Figure 4** – Example how the scaling factor M_{1i} is determined for the Hella station see Table 2.*

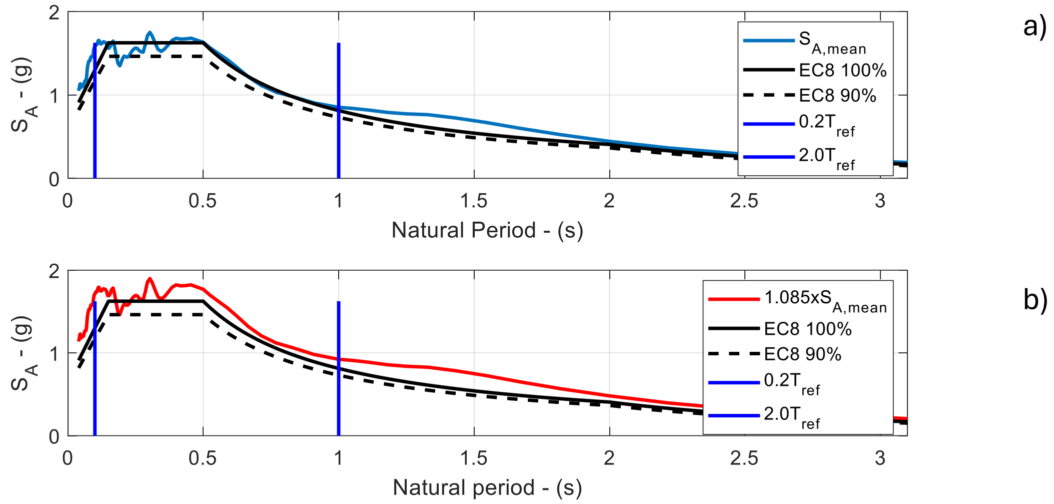

Figure 5 *– Example how the scaling factor M_2 is computed for T_{ref}=0.5s (M_2=1.085), see Table 3.*

At present state it is not known what reference natural period, T_{ref}, should be used for bridge so this process needs to be redone when modal analysis has been carried out for the bridge.

Since the scaling is referring to the horizontal component with the larger intensity the mean spectrum for the other component with the lower intensity is providing less seismic actions to the structural system. In a 3D time-history analysis using the scaled time histories two main load cases will be considered:

1. The time series with the larger intensity components (see Table 2) **acting in the longitudinal axis of the bridge** and the weaker components acting in the transvers direction. The scaling shall be based on reference natural period corresponding to the mode with the largest mass participation in the longitudinal direction.

2. The time series set with the larger intensity components (see Table 2) **acting in the transverse axis of the bridge** and the weaker components in the longitudinal direction. The scaling shall be based on reference natural period corresponding to the mode with the largest mass participation in the transvers direction.

In addition to run these two main cases. The sign of the acceleration time histories is reversed for each case, i.e. both using them as they are, a(t) and then as -a(t). This slightly affects the response.

2.4 Demand parameters and damage states

In seismic response analysis, demand parameters are quantitative measures of the response imposed on a structure by earthquake ground motion. They represent what the earthquake demands of the structure or structural element, as opposed to the structure or structural elements capacity. Displacement-based demand parameters are commonly used to predict damage. In this study the focus is on 1) the lead-rubber bearings (LRB) at the top of the piers and at the two abutments that support the superstructure, and 2) at the piers that are protected by the bearings against large horizontal seismic forces.

2.4.1 Lead-rubber bearings

Lead-rubber bearings can be of different height. Their weakest link is usually horizonal shear deformation, γ, which is defined as the ratio of their differential displacement between top and bottom of the bearing, Δ, dived with total rubber thickness, T_r of the bearing:

$$\gamma = \frac{\Delta}{T_r} \tag{3}$$

Based on this demand parameter four damage states are defined here for the lead-rubber bearings, see Table 4. To exceed a damage state, it is enough that a bearing passes the criteria in the table. As an example, if a bearing exceeds $\gamma = 50\%$, the bearings have has received a slight damage state etc.

***Table 4** – Definitions of damages states (DS) for lead-rubber bearings.*

DS	*Criteria*	Description of damage states
DS1	$0 < \gamma \leq 50\%$	No damage
DS2	$50\% < \gamma \leq 100\%$	Slight damage
DS3	$100\% < \gamma \leq 150\%$	Moderate damage
DS4	$150\% < \gamma \leq 200\%$	Severe damage
DS5	$\gamma > 200\%$	Very severe damage

2.4.2 Piers

The lead-rubber bearings reduce the horizontal seismic forces acting at the top of the piers. The maximum shear forces and bending moments caused by these forces are at the bottom of the piers where they are fixed to a rigid concrete foundation. By computing the yield moment and shear capacity at this cross-section it can be checked when the piers start yielding or exceeding their shear capacity.

2.5 Multi Scale Framework for Seismic Fragility Assessment

The seismic fragility of the Thjórsá bridge is quantified using a multi scale probabilistic framework that integrates system level response measures with localized component checks. The main focus is on the LRB and the isolation system. This hierarchical approach is adopted to ensure that global performance, governed primarily by the isolation system, is consistently reconciled with spatial variations in bearing demand across the arch deck configuration (Naeim and Kelly, 1999).

2.5.1 System Level Fragility: Global Envelope Approach

The primary stage of the assessment employs a Global Envelope Approach, in which the Engineering Demand Parameter (EDP) is defined as the absolute maximum shear deformation among the eighteen Lead Rubber Bearings (LRBs) during each nonlinear time history simulation. This formulation is motivated by three considerations.

- First, the maximum value envelope provides a worst case representation of isolation system demand, ensuring that the derived fragility curves capture the peak shear deformation irrespective of which support location governs the response (Choi et al., 2004).
- Second, because the deck behaves as a continuous diaphragm with strong load sharing characteristics, the performance of the overall system is typically controlled by the most highly stressed bearing, making the global envelope a practical surrogate for system level limit states (Nielson and DesRoches, 2007).
- Third, the approach introduces a conservative bias appropriate for safety critical structures, as it inherently accounts for the combined influence of arch anchorage, transverse frame interaction, and potential local irregularities in stiffness distribution.

2.5.2 Component Level Fragility: Localized Validation

To complement the system level assessment, a secondary component level fragility analysis is performed by independently evaluating the probabilistic demand distribution for each bearing. This localized analysis is particularly relevant for the Thjórsá bridge due to the presence of the rigid arch crown wall, which may induce non uniform demand patterns along the isolation interface. Comparison between component level and envelope based results enables identification of recurring critical locations, e.g., bearings adjacent to the arch or at abutment regions, and verifies whether the underlying capacity protected design philosophy is satisfied at all support points. This two tiered approach ensures that global performance metrics do not obscure potentially vulnerable components.

2.5.3 Directional Sensitivity and Ground Motion Grouping

Recognizing the significant influence of seismic orientation on bridge response, the input ground motion set is partitioned into two directional groups (see also the last paragraph if section 2.3).

Group 1: comprises records who's dominant (major) component aligns with the longitudinal axis of the bridge, whilst the les dominant (minor) component aligns with the transverse axis. This case is primarily assessing the efficiency of the arch–deck anchorage system.

Group 2: consists of motions whose dominant component acts transversely, providing insight into lateral stability and frame action.

This classification enables explicit evaluation of direction dependent fragility, which is particularly important for arch bridges exhibiting geometric and stiffness asymmetry.

2.6 Assessing fragility curves from IDA curves

A fragility curve represents the probability that an engineering demand parameter (EDP) exceeds a given damage state (DS) for given intensity measure (IM), which in our study is defined with Peak Ground Acceleration (PGA). The methodology can be described by Figure 6 which shows as a typical result from an IDA using non-linear time history analysis with stepwise increasing the intensity of the nine time series from PGA=0.1g to 1.0g. The figure shows ten stripes, one for each PGA level, with computed shear strains demands for each of the nine time series. The plot also shows the damage states as defined in Table 4. As an example, the PGA=0.1g stripe shows that none of the points exceeds the DS1 (No damage). For given stripe it is possible to define a probability model for the EDP, γ, based on the nine points for each stripe. This is shown schematically for the PGA=0.7g stripe where a lognormal probability function has been fitted to data points. With the provided probability model it is possible to predict the probability of exceeding any damage state shown on the figure, i.e. the vertical lines γ=(0.5, 1.0, 1.5 and 2.0). By repeating this approach for all the stripes we can construct independent probability model for each intensity level:

$$EDP\ |PGA_i \sim Lognormal(\mu_i, \theta_i) \qquad (4)$$

With these models the last step would be to derive and draw discrete fragility curves. The main limitations of this methodology are that the resulting fragility curves are not smooth and not described by two parameters which are common to see in the literature.

A useful refinement of the methodology is to assume a model that cover all the data points, i.e. pooling all the 90 points. Since the variability in EDP, i.e. γ, is increasing with intensity (see Figure 8) it is common to us a regression in log-log space where it is assumed that relative variability (coefficient of variation) is roughly constant for all intensity levels:

$$\ln(EDP) = a + b \cdot \ln(IM) + \varepsilon\,, \quad where\ \varepsilon \in N(0, \sigma) \qquad (5)$$

This model assumes that ln(EDP) is normal distributed with the mean: $a + b \cdot \ln(IM)$ and the standard deviation σ. This methodology is the same as in used in cloud-analysis, since in both cases all data points are pooled and used in the regression to compute *a, b* and σ.

Now the fragility curves for each damage stage are found by computing the probability of exceeding the four defined damage states which boundary is given by the vector $\gamma_i = [0.5,\ \ 1.0,\ \ 1.5,\ \ 2.0]$ see Table 4. That is

$$\mathrm{P}(ln(EDP) > ln(\gamma_i)\ |\ IM) = \Phi\left(\frac{a + b \cdot ln(IM) - ln\,(\gamma_i)}{\sigma}\right) \qquad (6)$$

This formula can be transformed to common formulation of fragility curves which are function of PGA which is used as IM in this study:

$$\mathrm{P}(DS > ds_i)\ |\ PGA) = \Phi\left(\frac{ln(PGA) - ln(\alpha_i)}{\beta}\right) \qquad (7)$$

where β, the dispersion parameter, is the same for all the fragility curves, and α_i are given as:

$$\beta = \frac{\sigma}{b} \tag{8}$$

and

$$\alpha_i = exp\left(\frac{ln(\gamma_i) - a}{b}\right) \tag{9}$$

where *a, b* and σ are the regression parameters. Other variants of the regression analysis exist but are not discussed here

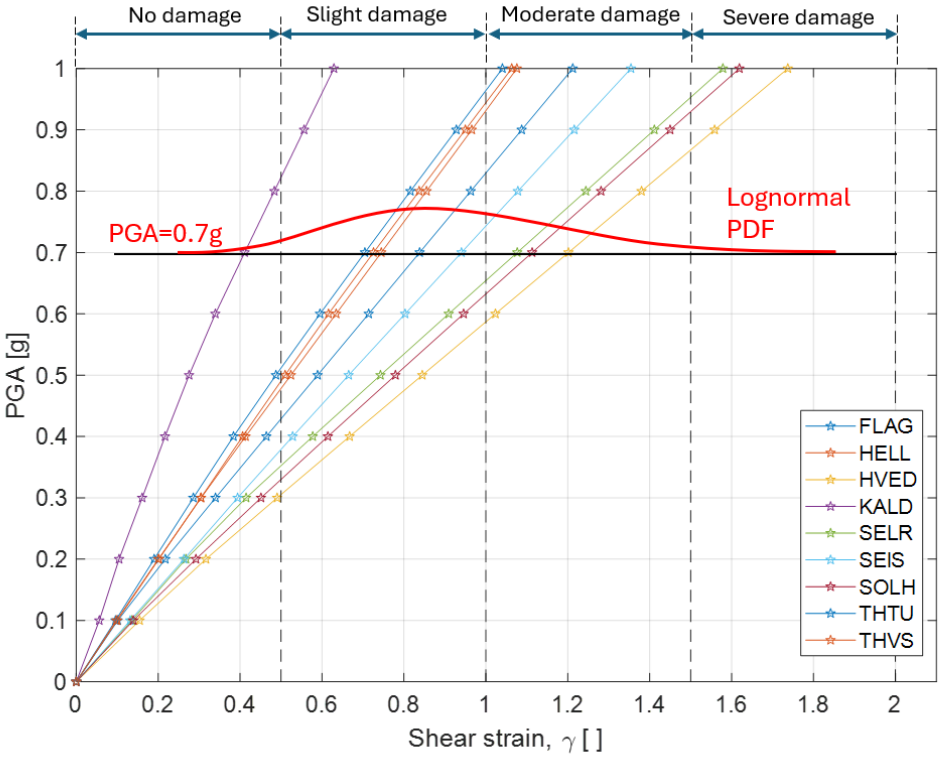

***Figure 6** – IDA curves computed with non-linear time history analysis for nine series as given in the legend. The damage states are marked on the plot at the top.*

In this study, both the first method mentioned above where each stripe was treated separately, and a variant of the regression method with pooling the data were used. The results were compared and showed to be quite similar. In the result chapter of this report (chapter 4), only results based on pooling the data are shown.

3 Numerical Modelling and Analysis

The numerical simulation of the Thjórsá bridge follows a capacity-based design philosophy where the superstructure is intended to remain largely undamaged during seismic events. Following the methodology suggested by Furinghetti et al. (2023), the bridge deck is modelled using elastic frame elements. This simplification is justified by the fact that deck systems in isolated bridges typically exhibit an elastic response, as the seismic energy is concentrated and dissipated within the isolation layer and the piers, which are the more vulnerable components. A simoilar elastic approach has been applied to the modelling of the abutments.

3.1 Description of the Thjórsá-Bridge

The case study is the Thjórsá-Bridge, an essential infrastructural connection traversing the Thjórsá river within the SISZ. The bridge is a composite steel and concrete structure measuring 170 meters in total length as shown in Figure 7.

- Superstructure and Arch: The superstructure (the deck) is supported with both the arch and the piers. The arch is extending 78 meters across the main river current (Figures 7 and 8). A critical feature of the design is the concrete wall at the arch crown (indicated in yellow on Figure 8a). This crown wall provides a rigid, monolithic connection between the arch and the deck at a 27 m long section ensuring the arch offers the primary longitudinal stability for the entire structure. Both the superstructure and the arch have a composite steel concrete cross-section (Figure 8b).
- Substructure and Abutments: The deck is sustained by seven concrete piers (Súla 1 to Súla 7 on Figure 7) and two terrestrial abutments. The piers consist of two columns that are connected at the top with transverse cap beam. The longest piers also have tie-beam at the middle-height (see Figure 1)
- The abutments utilize reinforced concrete walls to provide high boundary stiffness. While the crown is a rigid anchor, the other support points employ an isolation method to maintain flexibility under dynamic loads and provide seismic protection for the piers.
- Seismic Protection: Seismic protection is achieved by installing Lead Rubber Bearings (LRBs) at the interfaces between the piers and the superstructure.

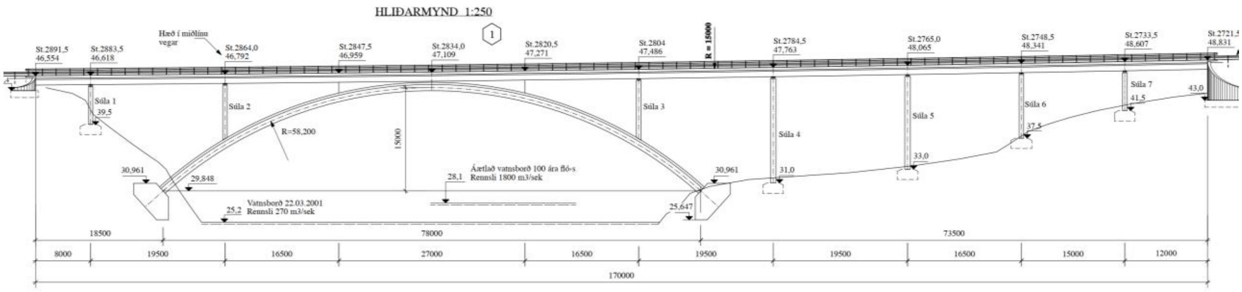

__Figure 7__ – Side view of the Thjórsá-Bridge (Vegagerðin, 2002).

a)

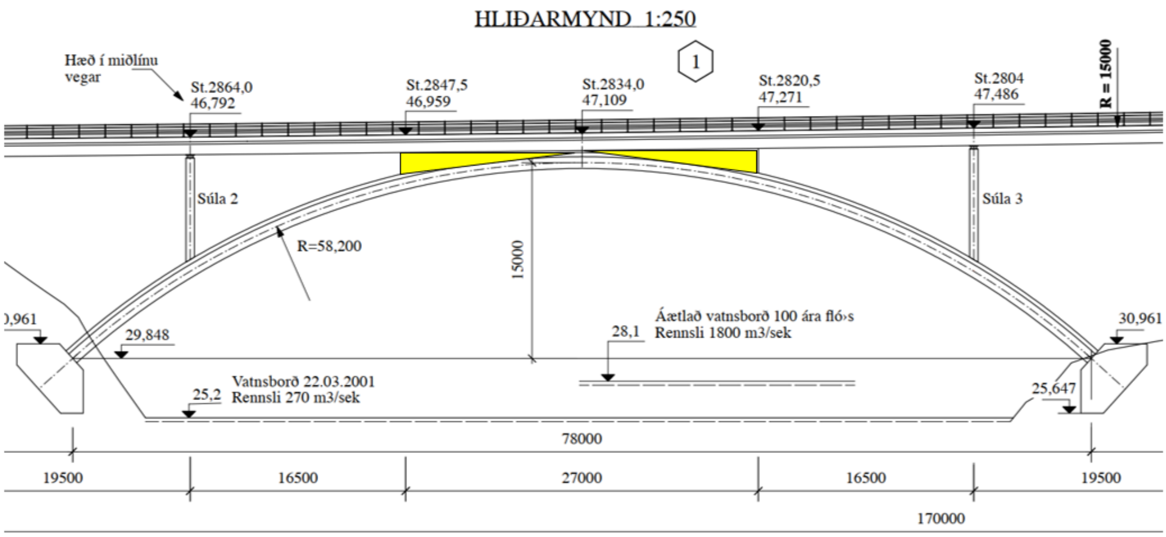

b)

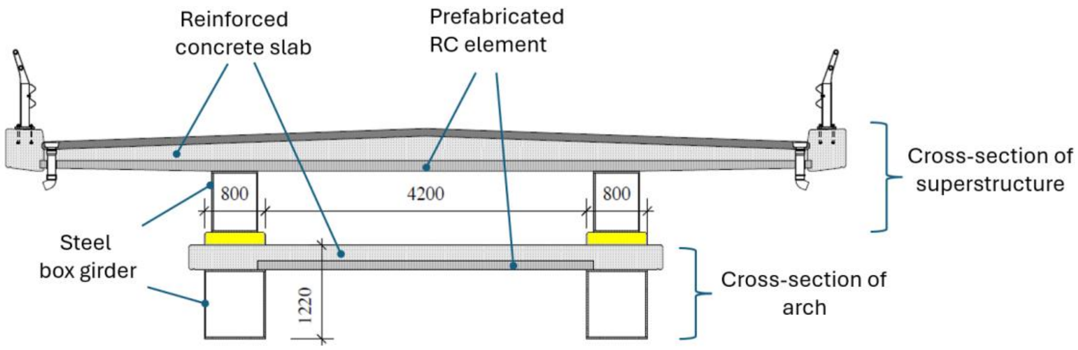

***Figure 8** – a) Side view of the arc showing the 27 m long crown wall (yellow) connecting the superstructure and the arch. b) Section view of superstructure and the arch at the top point of the arch. Both the superstructure (the deck) and the arch have composite steel concrete cross section. The crown wall is yellow. Modified version of the technical drawings from Vegagerðin (2002)*

3.2 Description of the SAP2000 model

The bridge was modelled using the finite element software SAP2000 to perform both modal and nonlinear time-history analyses. The model is a full three-dimensional (3D) representation designed to capture the interaction between the arch, the deck, and the isolation system as shown in Figures 9 and 10.

- Structural Elements:
  The composite steel concrete deck was modelled using shell and frame elements to accurately capture the stiffness and mass distribution. The shell elements represent the concrete slab, with their mid-plane positioned at the centre of the slab thickness. The longitudinal frame elements represent the steel

box girders, with their centroids aligned with the geometric centre of the steel section.

To maintain the physical offset and ensure full composite action between these components, vertical rigid links were employed to connect the shell element nodes to the frame element nodes (Figure 8b). The same model procedure is used to model nodes the arch. This modelling technique correctly accounts for the eccentricity of the sections and the resulting transformed moment of inertia. The same procedure was applied to the modelling of the arch-deck interface. The central arch and concrete piers were modelled using 3D frame elements, with sectional properties assigned to match the as-built geometry.

- Transverse beam connectivity conditions:

  In the analysis, two models were considered for the transverse beams connecting the longitudinal steel box girders in superstructure and the arch as well as in the transverse beams connecting the two columns in the piers:

  Pinned model, where the connections were pinned using end release for these beams. In this configuration, the beams transfer only shear and axial forces, representing a more flexible superstructure where lateral loads are primarily resisted by the individual stiffness of the piers and the arch.

  Fixed model, where the transverse beams are rigidly connected to the longitudinal girders and columns in the piers. This creates a moment-resisting frame effect across the bridge width, significantly increasing the torsional and transverse stiffness of the deck and allowing for a more integrated structural response. It is believed that this model is more realistic.

- Seismic Isolation (LRB):

  The LRBs were modelled using Nonlinear Link Elements. A bilinear hysteretic model was applied to these link elements to simulate the yielding of the lead core and the subsequent energy dissipation (see Figure 11).

- Boundary Conditions:

  All pier and arch footings were assigned fixed supports, reflecting the high-stiffness connection to the basaltic bedrock. The seismic input was applied as ground acceleration time-histories at these base nodes.

- Mass and Damping:

  The seismic mass was derived from the self-weight of the structural elements plus a portion of the superimposed dead loads. Rayleigh damping was utilized to account for the inherent energy dissipation of the materials, typically assumed at 5% for the primary modes of vibration.

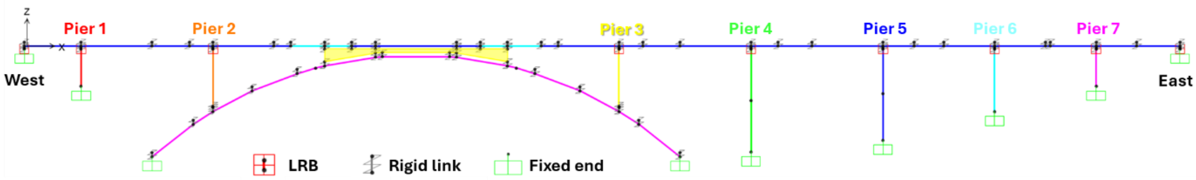

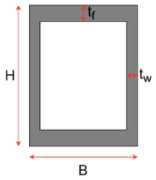

	Arc	Girder	Girder	TransBeam	TransBeam Arc
H	900	800	800	500	630
B	800	600	600	400	400
t_f	25	22.5	32.5	12	15
t_w	20	15	15	12	15

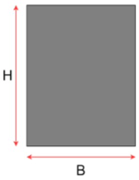

	TransBeam			
	P1/P7	P4/P5 B[1]	P4/P5 T[2]	P2/P3/P6
H	900	900	900	900
B	550	700	700	550
A_s	2165	4619	3637	3147

1) Beam at middel-height
2) Beam at top

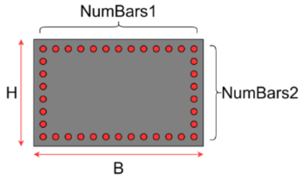

	Pier 1	Pier 2/3/6	Pier 4/5	Pier 7
H	650	650	800	650
B	1000	1000	1000	1000
NumBars1	13	11	8	9
NumBars2	8	8	10	8

All dimensions in mm

***Figure 9** – The Thjórsá-Bridge: Side view of the SAP2000 model showing details of the cross-sections in girders, arch and piers, as well as their transverse beams.*

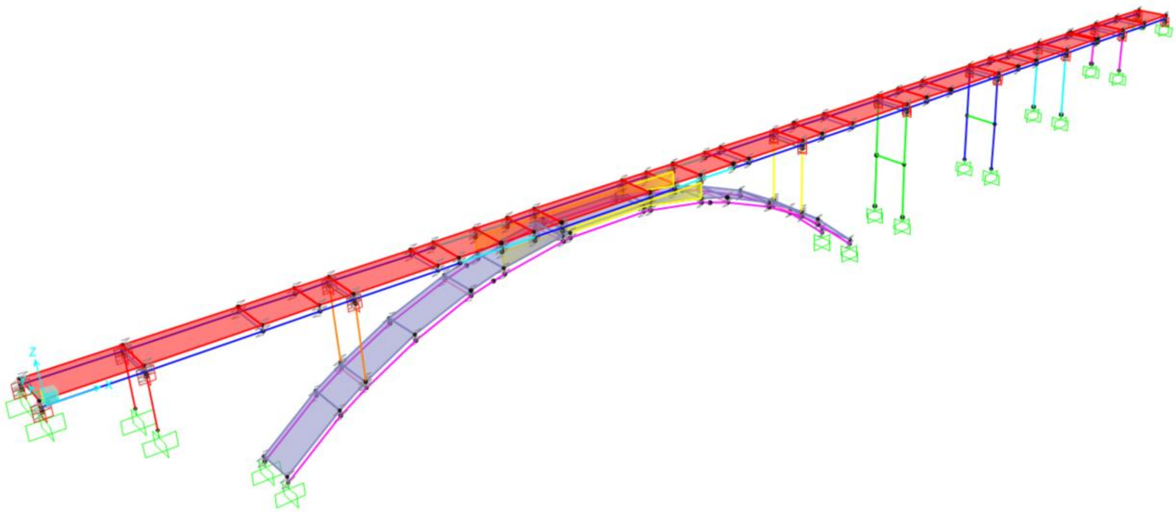

***Figure 10** – 3D SAP2000 model of the Thjórsá-Bridge.*

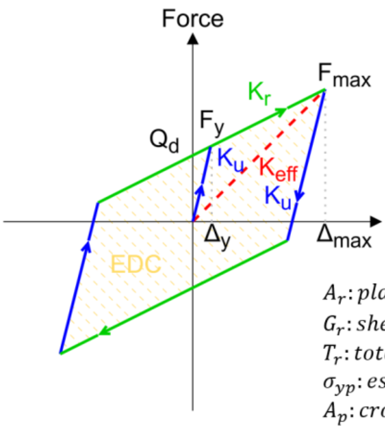

$$K_d = K_r = \frac{A_r G_r}{T_r}$$

$$K_u = 11.6 K_r$$

$$Q_d = \sigma_{yp} A_p$$

$$K_{eff} = \frac{F_{max}}{\Delta_{max}} = \frac{Q_d}{\Delta_{max}} + K_r$$

Stiffness	Φ450 ×156	Φ500 ×156
	Type 2 – Lead core Φ120 (MN/m)	
K_u	19.5	24.4
$K_{70\%}$	3.14	3.56
$K_{200\%}$	2.19	2.62
K_r	1.68	2.10

A_r: *plane area*
G_r: *shear modulus*, $1.00\ MPa$
T_r: *total thickness of the rubber in the bearing*, $88mm$
σ_{yp}: *estimated effective yield shear stress of the lead plug*, $8.0MPa$
A_p: *cross – sectional area of the lead plug*

***Figure 11** – Bilinear model of a Lead rubber bearing and the parameters used in the analysis.*

4 Results and discussion

This section presents the findings from the numerical simulations and evaluates the seismic performance of the Thjórsá bridge. The analysis progresses from a fundamental dynamic characterization of the structure to a probabilistic assessment of its vulnerability. First, a modal analysis is conducted to understand the sensitivity of the bridge's natural periods to the varying stiffness of the isolation system. Subsequently, the structural capacity is defined through specific limit states for the LRB. Finally, these results are synthesized into fragility curves, providing a statistical measure of the probability of exceeding damage thresholds under increasing seismic intensity levels.

4.1 Modal analysis and effective stiffness (K_{eff})

A modal analysis, which assumes that all elements are linear elastic, was performed to evaluate the dynamic characteristics of the Thjórsá bridge. Because the bridge relies on the LRBs for seismic isolation, its natural periods are not static; they shift significantly as the bearings transition from their initial elastic state which covers the situation for low amplitude vibrations to higher levels of plastic deformation.

4.1.1 Influence of Bearing Stiffness (K_{eff})

To capture this nonlinear behaviour, the first 12 natural periods were calculated for four distinct effective stiffness values (K_{eff}) representing critical stages of the bearing's hysteretic cycle (see Figure 11):

- Initial Stiffness (K_u): Represents the near-rigid elastic state before the lead core yields. This state corresponds to low-level ambient vibrations, traffic loads and wind loads.
- 70% Displacement Stiffness ($K_{70\%}$) corresponds to $\gamma = 70\%$: An intermediate seismic demand where the lead core has yielded, but the bearing has not reached serious damage states.
- 200% Displacement Stiffness ($K_{200\%}$): Corresponds to high-intensity demand, characterizing the "softened" state where period elongation is most pronounced.
- Post-Yield Stiffness (K_r): The tangent stiffness of the rubber and steel laminate. This value is critical for understanding the fundamental period during major seismic excursions.

4.1.2 Results and Mode Switching

The results for the first 12 periods across all eight scenarios are summarized in Table 5. The data shows a significant shift in the fundamental periods as the stiffness decreases from K_u to K_r.

A notable mode switching phenomenon occurs between the initial elastic state (K_u) and the yielded states. In the elastic range, the fundamental mode (Mode 1) is longitudinal. However, as the LRBs soften, the transverse direction becomes the most flexible, shifting the primary transverse vibration to Mode 1 for the remaining cases.

***Table 5** – Definitions of damages states for lead-rubber bearings. Natural periods of the first 12 modes under varying bearing stiffness stages (k_{eff}) and transverse beam connectivity conditions.*

Mode #	Pinned model				Rigid model			
	K_u (s)	$K_{70\%}$ (s)	$K_{200\%}$ (s)	K_r (s)	K_u (s)	$K_{70\%}$ (s)	$K_{200\%}$ (s)	K_r (s)
1	0.865	1.054	1.160	1.263	0.793	0.956	1.079	1.192
2	0.793	0.905	0.919	0.933	0.716	0.905	0.919	0.928
3	0.597	0.833	0.893	0.929	0.508	0.816	0.879	0.920
4	0.413	0.608	0.653	0.682	0.413	0.597	0.643	0.673
5	0.373	0.433	0.444	0.450	0.354	0.424	0.436	0.443
6	0.344	0.418	0.419	0.420	0.344	0.418	0.419	0.420
7	0.306	0.346	0.373	0.400	0.295	0.346	0.373	0.400
8	0.261	0.336	0.373	0.400	0.261	0.336	0.347	0.357
9	0.233	0.335	0.347	0.360	0.233	0.305	0.335	0.347
10	0.215	0.309	0.340	0.357	0.210	0.262	0.284	0.300
11	0.210	0.305	0.335	0.357	0.210	0.260	0.262	0.267
12	0.207	0.305	0.335	0.347	0.207	0.237	0.254	0.264

4.1.3 Modal Mass Participation and Higher-Order Effects

The distribution of modal mass reveals how different structural components respond to seismic excitation in longitudinal, transverse and vertical direction of the bridge. For seismic loads, the two horizontal directions are of main concern:

- **Longitudinal direction:** Depending on the K_{eff} and model type (Pinned or Fixed) the mode 1, 2 or 3 have the largest contribution for this direction, where the modal mass participation factor is in the range 0.40 to 0.41. The accumulated sum for the first 12 modes is in the range 0.45 to 0.71.

- **Transverse direction:** Similarly, depending on the K_{eff} and model type, mode 1 or 2 have the largest contribution for the transverse direction. Here, the modal mass participation factor is higher than in the longitudinal direction, ranging from 0.44 to 0.76. The accumulated sum for the first 12 modes is between 0.83 and 0.88, confirming that the primary seismic demand is concentrated in the low-frequency range, effectively managed by the isolation system.

- **Significance of Higher-Order Modes (Modes 4–12):** Although these modes account for less than 17% of the participating mass, they represent critical structural behaviours. As illustrated in the first three dominant mode shape visualizations in Figure 12, the lower modes establish the global response, while higher-order modes involve coupled lateral swaying of the steel arch and transverse deformation of the deck.
    - Unlike simple vertical vibrations, these modes indicate that the arch and deck interact dynamically at higher frequencies.
    - This confirms that the arch is not merely a "passenger" on the deck but has its own lateral dynamic characteristics that could influence local stresses in the arch ribs and hangers during a seismic event.

Mode 1	Transverse view of Pier #5	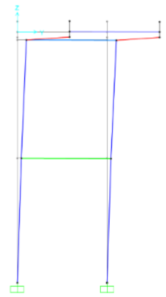
	Side view	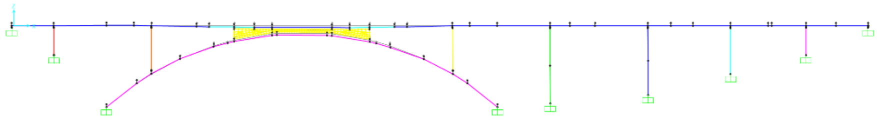
	Pan view	
Mode 2	Transverse view of Pier #5	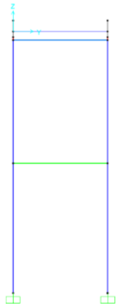
	Side view	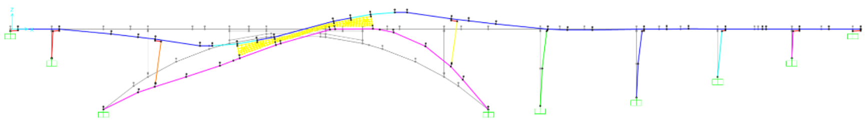
	Pan view	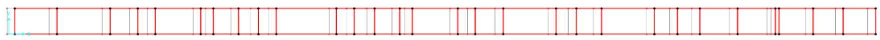
Mode 3	Transverse view of Pier #5	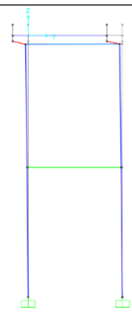
	Side view	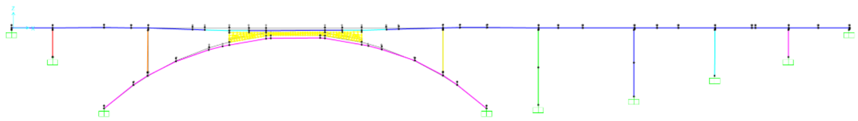
	Pan view	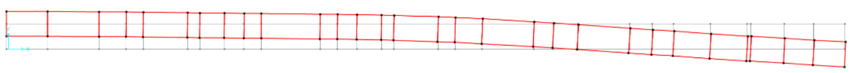

***Figure 12** – Transverse view (yz-plan) for pier #5, side view (xz-plan) and plan view (xy-plan) for Mode 1, 2 and 3 for the Rigid model and $K_{70\%}$.*

4.2 Scaling of time histories

From Table 5 it can be seen that for the both models (Pinned and Fixed) and considering only $K_{70\%}$ and $K_{200\%}$ the natural periods for modes 1, 2 and 3 are in the range 0.82 s to 1.16 s. Based on this period range, the reference period for the scaling method explained in section 2.3 is selected to be T_{eff} =1.0 s. This period and the dominating component for each station as computed by Eq.(1) is used to fit the elastic spectrum for the Thjórsá-bridge site. The target spectrum is defined in the National Annexes (NA) for Iceland (SI, 2010). That is a ground type A (rock) spectrum, which for an importance factor $\gamma_I = 1.0$, results in $a_g = 0.5g$. Furthermore, as defined in the NA, the spectral parameter for the near-fault areas in the SISZ is $T_c = 0.5s$. The scaling factors, M_{1i} and M_2 based on all this are given in Table 6 for the selected acceleration time histories.

Table 6 *– Scaling factors for the selected time histories for T_{ref}=1.0s for rock condition (Ground type A), a_g=0.5g and T_c=0.5s (SI, 2002). The second scaling factor is found to be M_2=1.071.*

No.	Date	Station	Dominating component	Unscaled PGA – (g)	M_{1i}	$M_i = M_{1i} \times M_2$	Scaled PGA – (g)
1	17.06.2000	HELL	Y	0.48	1.244	**1.332**	0. 64
2	17.06.2000	KALD	X	0.63	1.037	**1.111**	0.70
3	17.06.2000	FLAG	X	0.32	1.381	**1.479**	0.47
4	21.06.2000	THBR	Y	0.84	0.848	**0.908**	0.76
5	21.06.2000	THTU	Y	0.57	0.960	**1.028**	0.59
6	21.06.2000	SOLH	Y	0.72	0.868	**0.930**	0.67
7	29.05.2008	SELR	X	0.54	1.338	**1.433**	0.77
8	29.05.2008	HVED	Y	0.47	1.188	**1.272**	0.56
9	29.05.2008	SELS	X	0.51	1.468	**1.572**	0.80
		Mean:		0.56		Mean:	0.66

In the incremental dynamic analysis, the intensity is scaled from 0.1g and up to 1.0g. Since the scaling shown in Table 6 refer to a_g=0.5g the scaling, as an example, for intensity a_g=0.1g, would require that each time history would be multiplied with $M_i \times 0.2$. Similarly, for a_g=0.2g with $M_i \times 0.4$, etc.

4.3 System level fragility curves for the Lead-Rubber bearings

The final stage of the assessment involves the generation of fragility curves. These curves represent the conditional probability that the structural demand (displacement) exceeds a specific limit state capacity at a given seismic intensity (*PGA*). By plotting these probabilities for both the longitudinal and transverse directions, we can identify the most vulnerable axes of the bridge and determine the intensity levels at which the risk of damage becomes critical for the Thjórsá-bridge's operational continuity.

The resulting fragility curves for the system level fragility (see section 2.5.1) are as shown in Figure 13. This figure provides a comparative visualization of the two motion groups across both longitudinal and transverse directions (Group 1 Dominate comp: Long and Group 2 Dominate comp: Tran). Each plot includes the median capacity (α) and dispersion (β) parameters for the four damage states (DS1-DS4), derived from the lognormal distribution of the maximum structural responses. As an example for the Rigid model (b), the probability of exceeding damage state 1 (DS1 – No damage) when the dominating action is in the longitudinal direction and the response under consideration is also in the longitudinal direction is ~30% at PGA=0.4g whilst the probability of exceeding DS2 (slight damage) is ~0%. The transverse direction is more critical and from figure most to right the probability of exceeding DS1 at PGA=0.4g is ~100%, and the probability of exceeding DS2 at PGA=0.4g is ~60%. On the other hand, the probability of exceeding DS4 (γ=200%, => exceed a displacement: $\Delta = 2 \times T_R = 172\ mm$) at PGA=0.4g is ~5%. From the technical drawings (Vegagerðin 2002) it can be seen that superstructure will impact the wing walls at the abutments at a transverse displacement of 200 mm. So, this is not so critical. At PGA=0.5g the probability of exceeding DS4 is ~10%.

The dots on each graph on Figure 13 show the number of counts (time histories) that exceed a given damage state threshold: $\gamma_i = [0.5,\ \ 1.0,\ \ 1.5,\ 2.0]$ at each intensity level. For instance, for the graph on far left in Figure 13a, four time histories out of nine (4/9=0.44) scaled for PGA=0.4g exceed DS1(the blue curve). The dots indicate that the curves are fitting the data quite well. It would nevertheless be preferable to have more than nine time histories to use in the analysis, say 20 to 30.

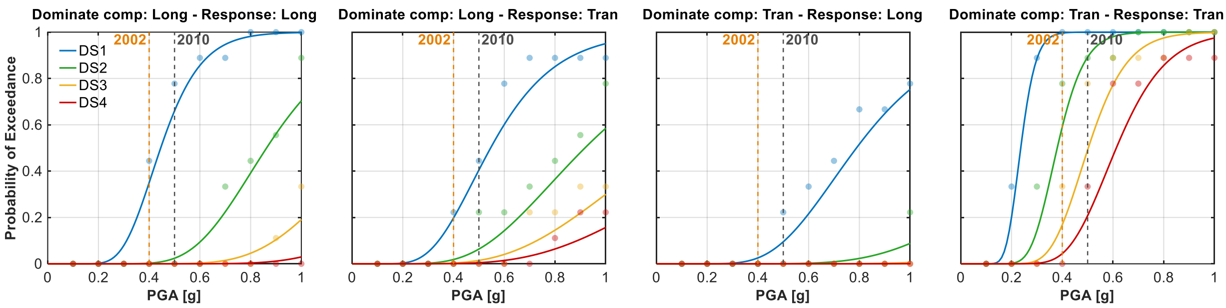

(a)

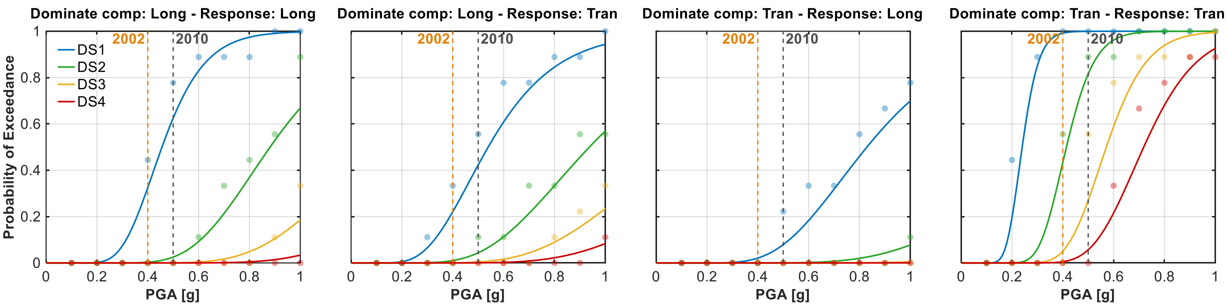

(b)

***Figure 13** – Fragility curve for the four damages stages defined in Table 4. The two vertical dashed lines show the reference peak ground acceleration, a_{gR}, on type A ground for a 475 year return period at the Thjórsá-bridge site as it was given in the National Documents with the Eurocodes in 2002 (SI, 2002) and in the National Annexes with the Eurocodes in 2010 (SI, 2010) : (a) End Moment Release (Pinned) and (b) No Release (Rigid).*

Furthermore, Figure 13 superimposes two vertical dashed lines that reflects the seismic hazard levels defined in 2002 by the Icelandic National Documents (SI, 2002), and in 2010 by the Icelandic National Annexes (SI, 2010). The reference peak acceleration, a_{gR} (PGA), on type A ground for a 475-year return period was increased form 0.4g in 2002 to

0.5g in 2010 in the SISZ. In addition, the T_c parameter, defining the upper limit of the period of the constant spectral acceleration branch, was increased from 0.4 s to 0.5 s that also increases the seismic loads for structures with long natural periods. This allows for a direct assessment of the bridge's performance relative to historical and modern safety requirements. As seen in the figure, the shift in code requirements significantly influences the probability of exceedance, particularly for the serviceability limit states (DS1 and DS2), providing a clear graphical representation of the bridge's safety margin evolution.

Fragility curves for the component level fragility (see section 2.5.2) are provided in Annex. That is fragility curves for each bearing in the bridge, starting at the west abutment (WA), individually for the north and south side bearings. Then pier-by-pier in the east direction ending at the east abutment (EA).

4.4 Load bearing capacity of the piers

The LRBs are designed to dissipate energy and lengthen the natural period of the structure, thereby reducing the seismic loads on the piers which should preferable be in the elastic range. The FE-model used in the vulnerability assessment of the LRB assumes that the piers and as well as all other structural elements than the LRBs stay in the elastic range when exposed to seismic loads at any level. It is therefore interesting to use the FE-model to compute the peak moments at the bottom of the piers to check if they exceed the yield moment capacity.

Each pier consists of two columns (see Figures 1 and 10). The computed moments in the two columns of a given pier are nearly identical in every load case; therefore, the results presented below refer to a single column. Table 7 summarizes the absolute maximum moments recorded for all the pier-columns at a seismic intensity of PGA=0.5g. These values represent the envelope of the highest demands captured across the nine-ground motion NLTHA for both M_2 which resists transverse loads, and M_3 which resist loads in the acting in the longitudinal direction (see Figure 14).

For comparative assessment, the yield moment capacities ($M_{2,Y}$ and $M_{3,Y}$) were determined using the CUMBIA Matlab code (Montejo & Kowalsky, 2007). This utility performs a monotonic moment-curvature analysis of reinforce concrete members with rectangular section including the effect of axial load. The material properties of the concreter are based on the Mander model (Mander et al. 1988). Material properties of steel bars and concrete, as well as cross-section details are adopted from the technical drawings of the Thjórsá-bridge (Vegagerðin, 2022).

The results indicate that a seismic level corresponding to PGA = 0.5g, the column capacity (yield moments) significantly exceeds the computed demand moments. This confirms that the substructure remains well within the elastic regime, validating the modelling assumptions and demonstrating the effectiveness of the isolation system in protecting the primary vertical members.

***Table 7** – Demand moments M_D for PGA=0.5g and yield capacity moments M_Y in pier-columns for both M_2 and M_3 (see Figure 14).*

	Pier-1	Pier-2	Pier-3	Pier-4	Pier-5	Pier-6	Pier-7
$M_{2,D}$ – (MNm)	1.23	1.94	2.13	2.78	2.63	2.09	1.23
Time history	HveD	SelS	SelS	HveD	Solh	Solh	HveD
$M_{2,Y}$ – (MNm)	4.15	3.93	3.90	3.67	3.62	3.92	3.57
$M_{3,D}$ – (MNm)	1.26	1.56	1.49	1.67	1.90	1.49	1.34
Time history	Solh	HveD	HveD	HveD	HveD	HveD	SolH
$M_{3,Y}$ – (MNm)	2.68	2.43	2.41	2.79	2.76	2.45	2.17

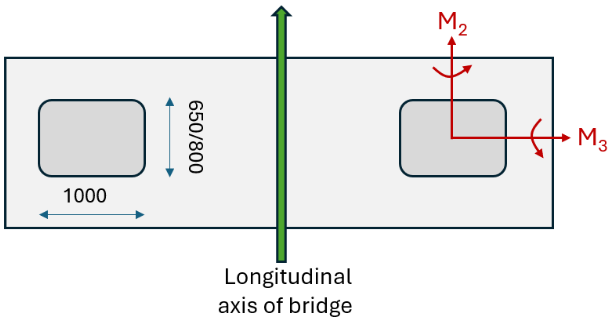

***Figure 14** – Plan view of the bottom part of pier consisting of fundament and two columns. The dimensions of column cross-section are either 1000x800 mm or 1000x650 and the reinforcement is different (Vegagerdin 2002). The M_2 moment is resisting loads in transverse direction and M_3 loads in longitudinal direction.*

5 Conclusions

This study evaluated the seismic vulnerability of the lead-rubber bearings (LRBs) at the top of the piers and the abutments that support the superstructure. Fragility curves have been evaluated for these components, and the most exposed bearings have been identified.

Scaled strong motion data from nine ground stations recorded in the South Iceland earthquakes in June 2000 and in May 2008 have been used as seismic loads in non-linear time history analysis of the bridge. Incremental dynamic analysis was applied by scaling selected set of the time histories. The intensity of the records are calibrated with the EC8 ground type A (rock) response spectra, for design ground acceleration, a_g, in the range 0.1g to 1.0g. Here, it can be noted that design acceleration for the Thjórsá-bridge site is 0.5g for the reference 475-year return period according to the National annexes for Iceland.

The investigation compared two structural configurations: 1) a "Pinned" model with moment end-releases on transverse beams in the cross-section of both the superstructure and the arch and 2) a "Fixed" model were all these transverse beams hand fixed connections (no end-releases). Furthermore, the influence of ground motion directionality was explicitly accounted for by partitioning the records into two groups:

- Group 1 (G1): Dominating seismic components acting longitudinally.
- Group 2 (G2): Dominating seismic components acting transversely.

Each set of ground motion data from a given station has two horizontal components and one vertical component. The more intense horizonal component in each set (either x- or y-component) were used as the dominating (major) component and the other as minor component. The major components were used in the scaling procedure and the obtained scaling factor then used to scale both the major and the minor components. Based on this thermology the FE-models were ran for two cases: G1 All the major components, scaled for specified a_g level, were acting in the longitudinal direction and all the minor components in the transverse direction; and G2 Vice versa, all the major components acting in the transverse direction and the minor components in the longitudinal directions.

Key findings from the study include:

- **Isolation Effectiveness**: The LRB system demonstrated high efficacy in protecting the substructure. The pier moment capacity checks confirmed that even at the design level of 0.5g, the piers remain well within the elastic range, validating the capacity-protected design philosophy.
- **Vulnerability Trends**: The fragility curves revealed that G2 motions (tranverse) generally impose higher displacement demands on the bearings compared to G1 in, highlighting the sensitivity of the arch-deck anchorage system to transverse excitation.
- **Code Evolution**: By superimposing the 2002 and 2010 Icelandic code requirements, the study illustrated a marked increase in the probability of exceeding serviceability damage states under modern standards, emphasizing the importance of periodic re-evaluation of existing infrastructure.

While the primary focus of this research was the isolation system, the multi-scale probabilistic framework developed herein is highly adaptable. Future vulnerability analyses can extend this methodology to other critical components, such as the steel arch ribs, superstructure cross-sections, and the bedrock anchorage system, to provide a comprehensive seismic risk profile for the entire bridge system.

References

CEN (2004) Eurocode 8: design of structures for earthquake resistance: part 1: general rules, seismic actions and rules for buildings, European standard. European Committee for Standardization, Brussels.

CEN (2005) Eurocode 8: design of structures for earthquake resistance: part 2: Bridges, European standard. European Committee for Standardization, Brussels.

Choi E, DesRoches R, Nielson B (2004) Seismic fragility of typical bridges in moderate seismic zones. Engineering Structures 26(2):187-199. https://doi.org/10.1016/j.engstruct.2003.09.006

Furinghetti M, Reale S, Fox MJ, Pavese A (2023) Numerical assessment of the seismic vulnerability of bridges within the Italian road network. *Applied Sciences 13*(14): 8194.

Jónasson K, Bessason B (2024) An earthquake catalogue for Iceland and the northern Mid-Atlantic ridge 1900–2023, Proceedings of the 18th World Conference on Earthquake Engineering, Milan Italy.

Jónasson K, Bessason B, Helgadóttir Á, Einarsson P, Guðmundsson GB, Brandsdóttir B, Vogfjörd KS, Jónsdóttir K (2021) A harmonised instrumental earthquake catalogue for Iceland and the Northern Mid-Atlantic ridge. Nat Hazards Earth Syst Sci 21(7):2197–2214. https://doi.org/10.5194/nhess-21-2197-2021

Mander JB, Priestley MJN, Park R (1988) Theoretical stress-strain model for confined concrete. Journal of Structural Engineering 114(8):1804-1826.

Montejo LA, Kowalsky MJ (2007) CUMBIA—Set of codes for the analysis of reinforced concrete members. CFL Technical Report No. IS-07-01, Constructed Facilities Laboratory, North Carolina State University, Raleigh, NC.

Naeim F, Kelly JM (1999) Design of Seismic Isolated Structures from Theory to Practice. John Wiley & Sons, Hoboken, 1999. http://dx.doi.org/10.1002/9780470172742

Nielson BG, DesRoches R (2007) Seismic fragility methodology for highway bridges using a component level approach. Earthq Eng Struct Dynamics 36(6):823-839. https://doi.org/10.1002/eqe.655

Padgett JE, DesRoches R (2008) Methodology for the development of analytical fragility curves for bridges in moderate seismic zones. Earthq Eng Struct Dynamics 37(8): 1151-1171. https://doi.org/10.1002/eqe.801

SI (2002) Icelandic National doucments to Eurocodes. Standards Council of Iceland/ Stadlarád Íslands (SI).

SI (2010) Icelandic National annexes to Eurocodes. Standards Council of Iceland/ Stadlarád Íslands (SI).

Vamvatsikos D, Cornell CA (2002) Incremental dynamic analysis. Earthq Eng Struct Dynamics 31(3):491– 514. https://doi.org/10.1002/eqe.141

Vegagerðin (2002). Technical drawings of the Þjórsá bridge on Road 1 in South Iceland, Icelandic Road and Costal Administration – Vegagerðin.

Annex - Component level fragility curves

Pinned model

(End-moment releases on transvers beams)

Fragility curves for different LRB starting at the West Abutments (WA) South side (S) and North side (N) bearing, and then moving to Pier 1 (P1-S) and P2-N), Pier 2, etc. and all the way to the East abutment south and north side bearings (EA-S) and (EA-N)

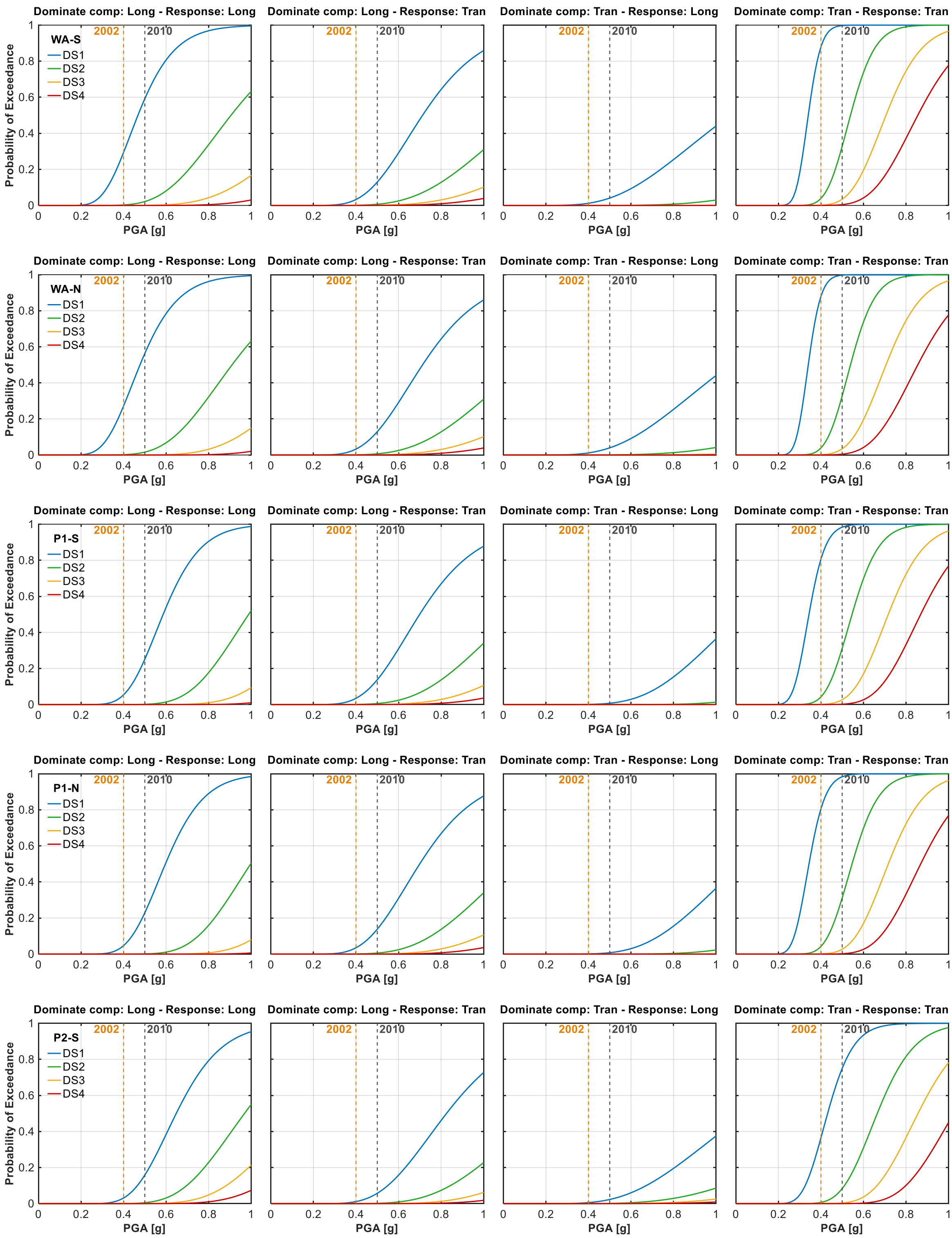

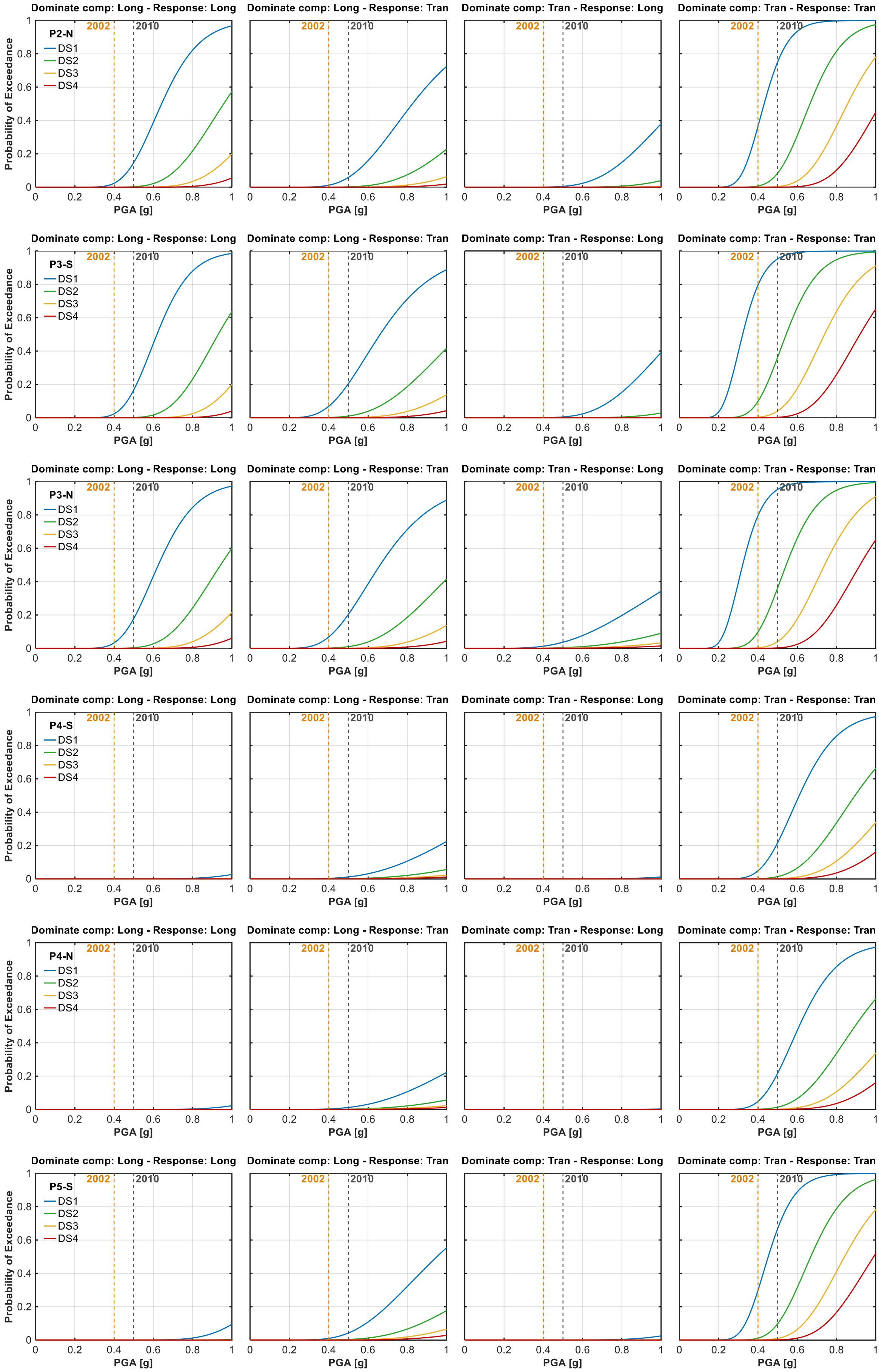
Dominate comp: Long - Response: Long
Dominate comp: Long - Response: Tran
Dominate comp: Tran - Response: Long
Dominate comp: Tran - Response: Tran
P2-N
P3-S
P3-N
P4-S
P4-N
P5-S
DS1
DS2
DS3
DS4
2002
2010
Probability of Exceedance
PGA [g]
0
0.2
0.4
0.6
0.8
1

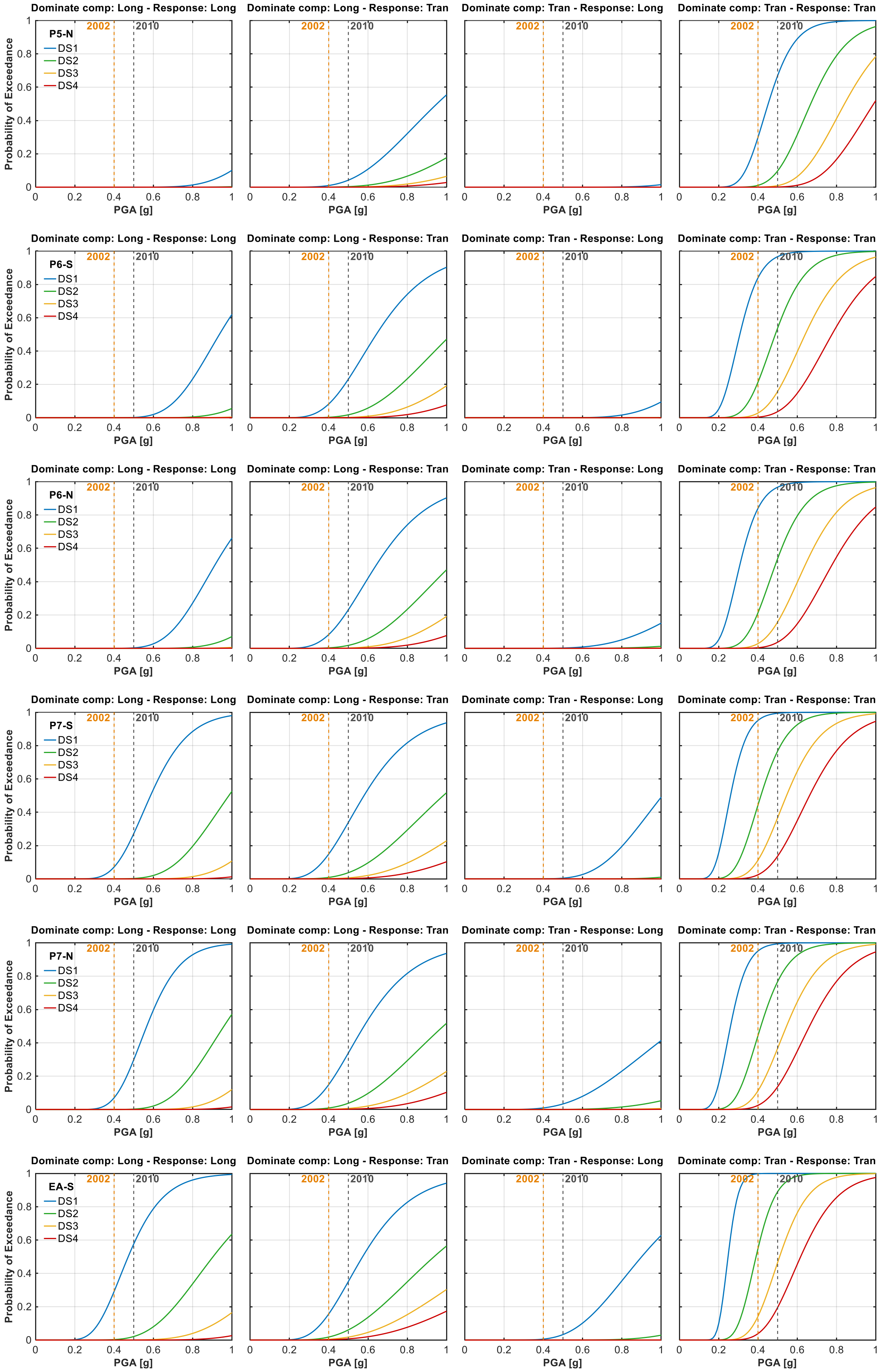
Dominate comp: Long - Response: Long
Dominate comp: Long - Response: Tran
Dominate comp: Tran - Response: Long
Dominate comp: Tran - Response: Tran
P5-N
P6-S
P6-N
P7-S
P7-N
EA-S
DS1
DS2
DS3
DS4
2002
2010
Probability of Exceedance
PGA [g]

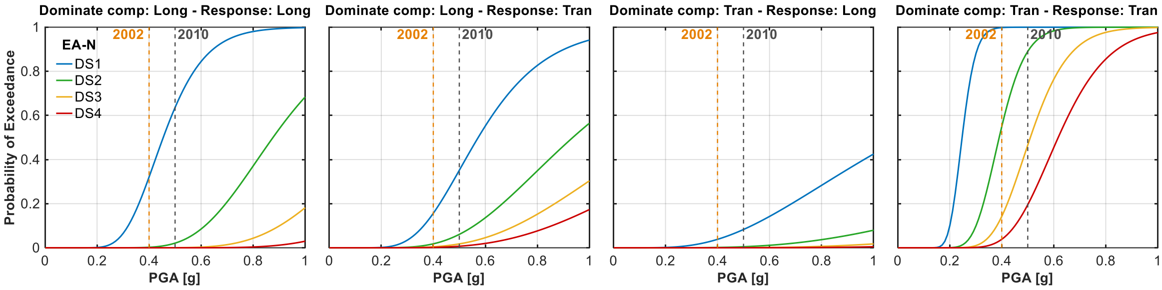

Fixex model

(No end-moment releases)

Fragility curves for different LRB starting at the West Abutments (WA) South side (S) and North side (N) bearing, and then moving to Pier 1 (P1-S) and P2-N), Pier 2, etc. and all the way to the East abutment south and north side bearings (EA-S) and (EA-N)

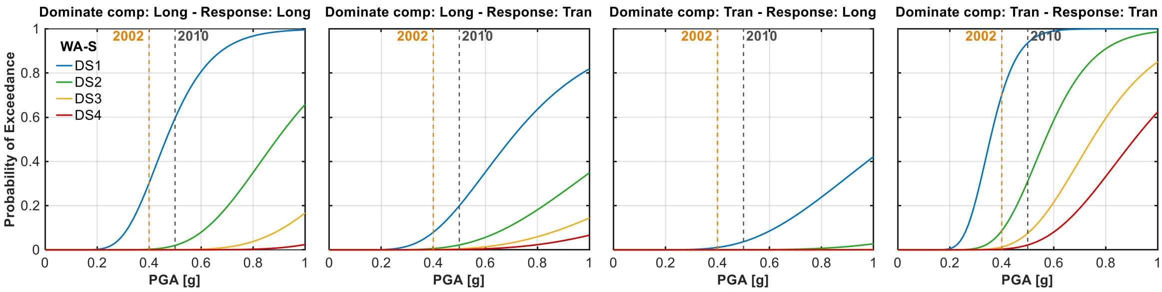

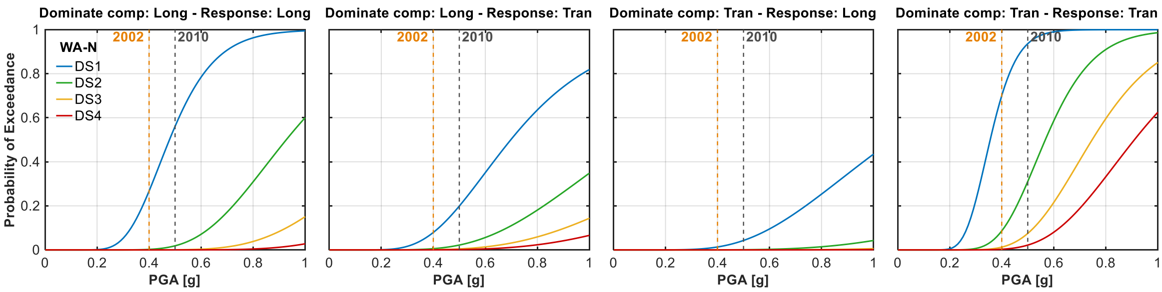

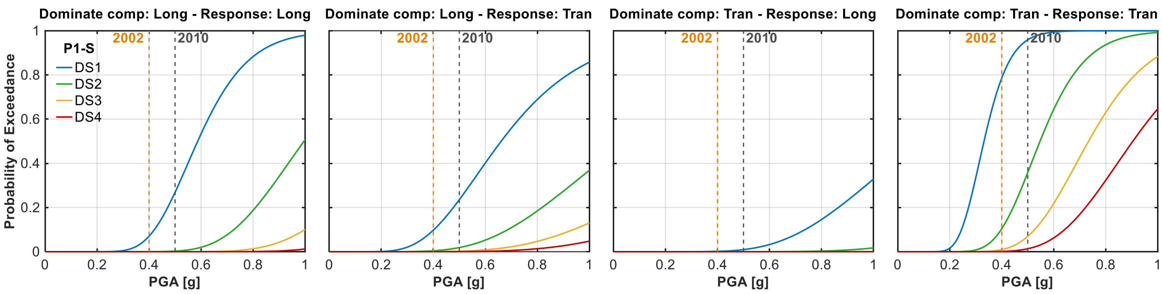

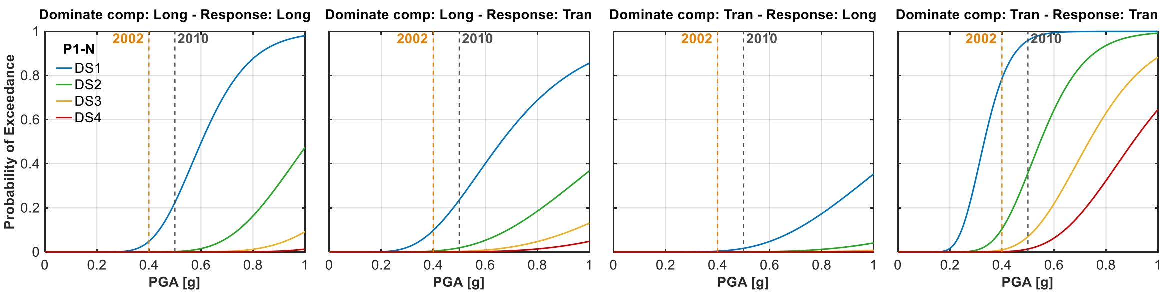

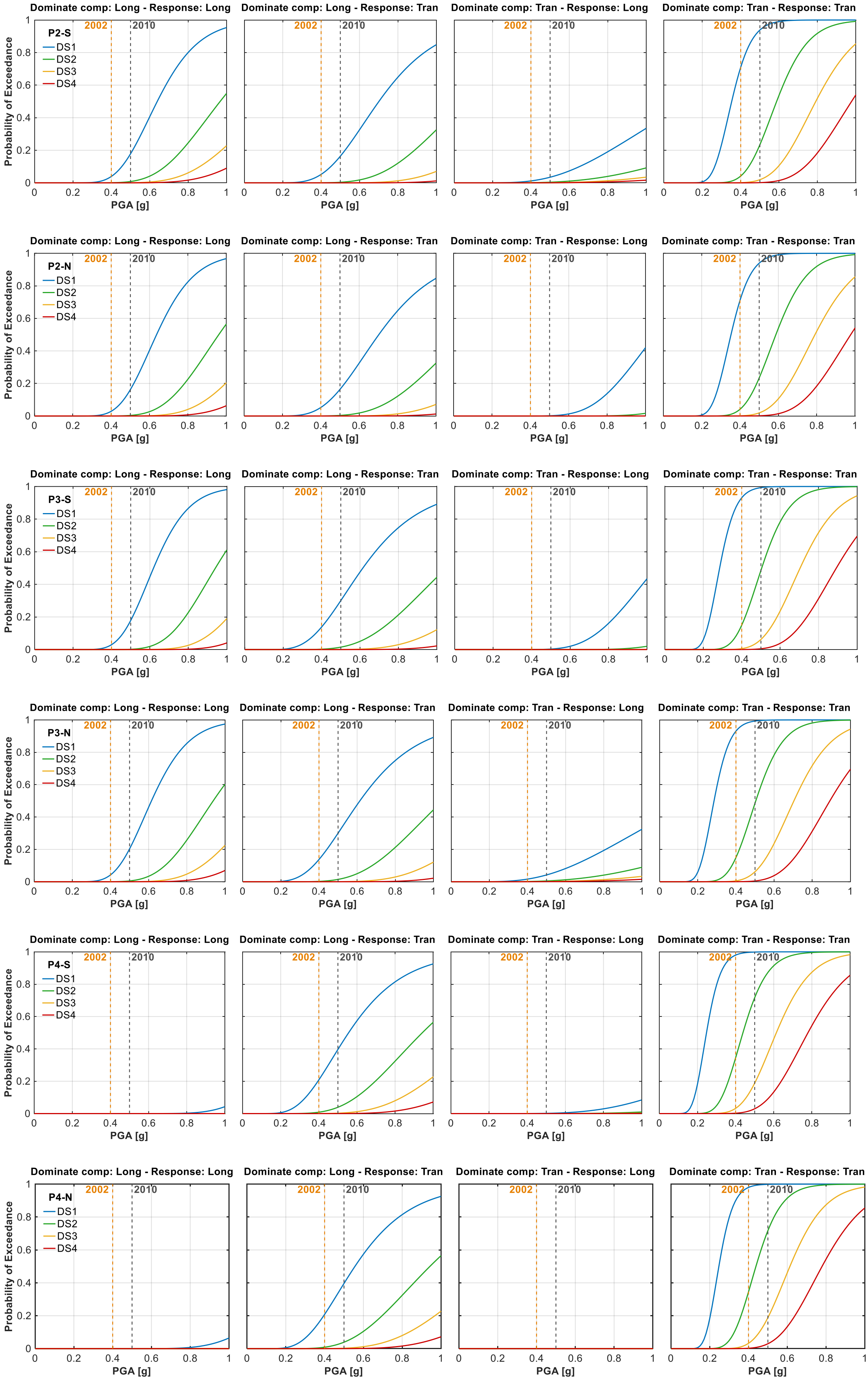
Dominate comp: Long - Response: Long
Dominate comp: Long - Response: Tran
Dominate comp: Tran - Response: Long
Dominate comp: Tran - Response: Tran
Probability of Exceedance
PGA [g]
2002
2010
P2-S
P2-N
P3-S
P3-N
P4-S
P4-N
DS1
DS2
DS3
DS4

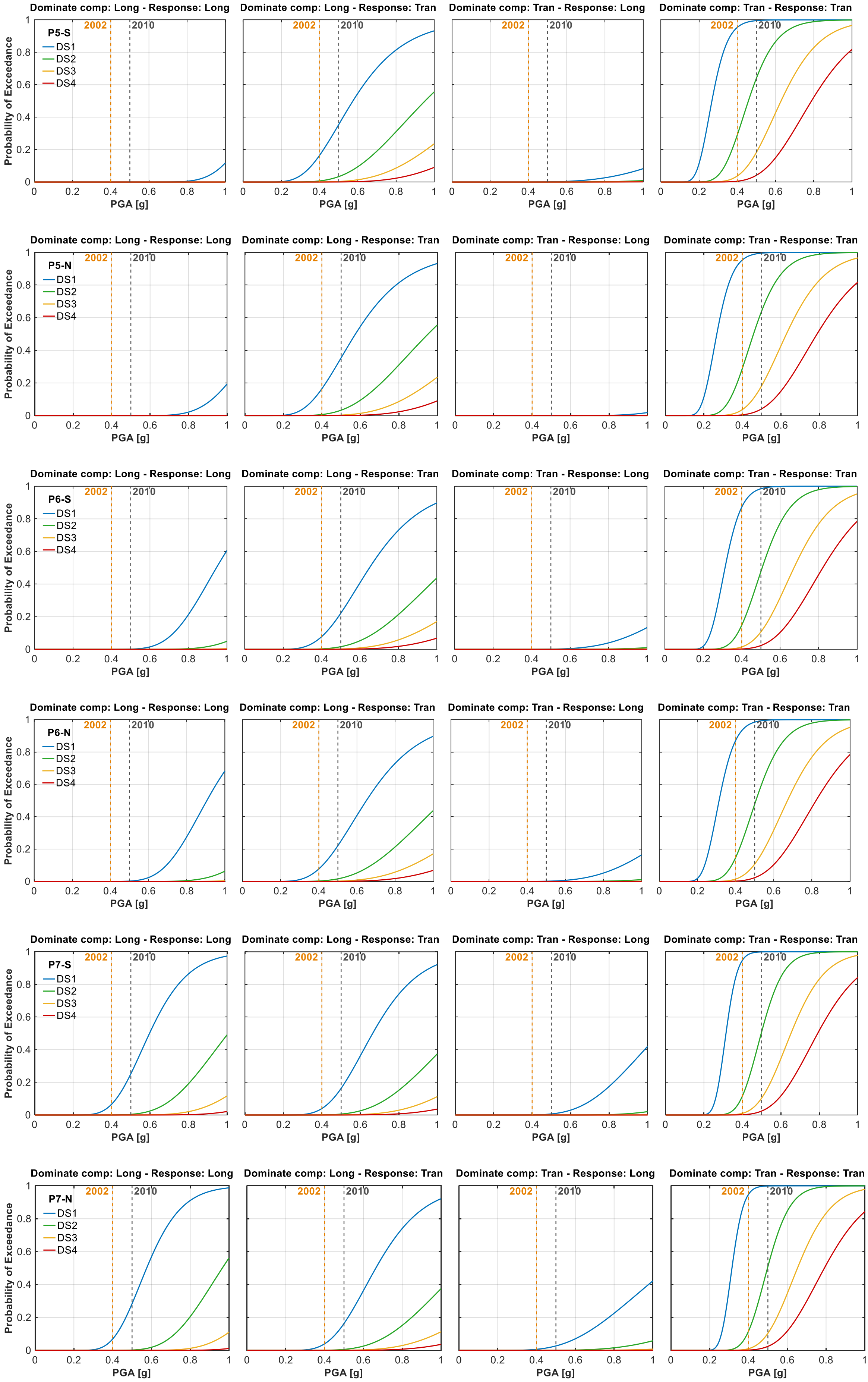
Dominate comp: Long - Response: Long
Dominate comp: Long - Response: Tran
Dominate comp: Tran - Response: Long
Dominate comp: Tran - Response: Tran
P5-S
P5-N
P6-S
P6-N
P7-S
P7-N
DS1
DS2
DS3
DS4
2002
2010
Probability of Exceedance
PGA [g]
0
0.2
0.4
0.6
0.8
1

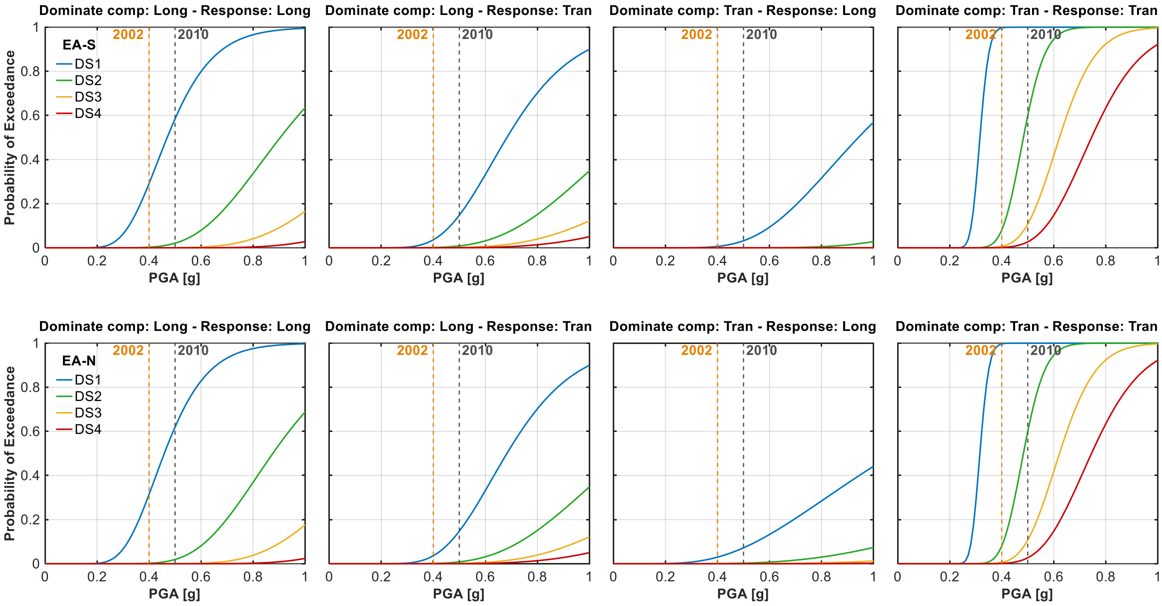
Dominate comp: Long - Response: Long
Dominate comp: Long - Response: Tran
Dominate comp: Tran - Response: Long
Dominate comp: Tran - Response: Tran
EA-S
EA-N
DS1
DS2
DS3
DS4
2002
2010
Probability of Exceedance
PGA [g]